METIS

Seismic Risk Assessment for Nuclear Safety

Research & Innovation Action

NFRP-2019-2020

Strategy for consideration of aftershocks in seismic PSA

Deliverable D7.4

Version N°5

Authors:

Dmytro Ryzhov (SSTC NRS)

Oleg Ponochovnyi (SSTC NRS)

Shadi Fathabadi (TUK)

Richard Styron (GEM)

This project has received funding from the Horizon 2020 programme under grant agreement n°945121. The content of this presentation reflects only the author's view. The European Commission is not responsible for any use that may be made of the information it contains.

Disclaimer

The content of this deliverable reflects only the author's view. The European Commission is not responsible for any use that may be made of the information it contains.

Document Information

Grant agreement	945121
Project title	Methods and Tools Innovations for Seismic Risk Assessment
Project acronym	METIS
Project coordinator	Dr. Irmela Zentner, EDF
Project duration	1st September 2020 – 31st May 2025 (57 months)
Related work package	WP7 - PSA Tools and Methodology
Related task(s)	Task 7.3.2 - Strategy for Consideration of Aftershocks in Seismic PSA
Lead organisation	SSTC NRS
Contributing partner(s)	SSTC NRS, TUK, GEM, ER
Due date	17th June 2023
Submission date	24th July 2024
Dissemination level	Public

History

Version	Submitted by	Reviewed by	Date	Comments
N°1	O. Ponochovnyi	I. Zentner E. Viallet	01/10/2022 15/02/2023	
N°2	D. Ryzhov	O. Sevbo E. Viallet I. Zentner	17/06/2023	
N°3	S. Fathabadi	I. Zentner O. Sevbo Robert Budnitz Nilesh Chokshi John Richards	21/12/2023 06/05/2024	
N°4	D. Ryzhov	Robert Budnitz Nilesh Chokshi John Richards	20/06/2024	
N°5	D. Ryzhov	I. Zentner O. Sevbo	24/07/2024	

Table of Contents

List of figures

List of tables

Abbreviations and Acronyms

Acronym	Description
AS	Aftershock
ABWR	Advanced Boiling Water Reactor
BWR	Boiling Water Reactor
CDF	Core Damage Frequency
DB	Database
DS	Damage State
EAB	External Advisory Board
FLEX	Diverse and Flexible Coping Strategies
HCLPF	High Confidence, Low Probability of Failure
MS	Mainshock
NPP	Nuclear Power Plant
PGA	Peak Ground Acceleration
PRA	Probabilistic Risk Assessment
PSA	Probabilistic Safety Assessment
PSHA	Probabilistic Seismic Hazard Analysis
RC-ESDOF	Reinforced Concrete (Structure) – Equivalent Single Degree of Freedom
RHR	Residual Heat Removal System
SPSA	Seismic Probabilistic Safety Assessment
SSC	System, Structure and Component
WWER	Water-Cooled Water-Moderated Power Reactor
WP	Work Package

Summary

This report focuses on the enhancement of the Seismic Probabilistic Safety Assessment (SPSA) procedure by accounting for additional seismic impacts caused by aftershocks on nuclear power plants (NPPs).

As part of this research, various references, databases, and internet sources were reviewed to evaluate experience feedback related to the effects of aftershocks on power plants' safety.

The strategy for considering aftershocks includes additions to key elements of the SPSA procedure, namely: seismic hazard analysis, fragility evaluation, and system analysis considering additional impact of aftershocks on possibly weakened structures, systems, and components (SSCs) of NPPs due to the mainshock. The scenario where the plant is being transferred into a cold shutdown state after an emergency shutdown resulting from the mainshock is also considered.

Keywords

Aftershock, mainshock, seismic PSA, seismic hazard, seismic fragility, system reliability analysis, event trees, fault trees, core damage frequency.

Introduction

Nuclear power plants are complex and critical structures comprised of numerous interdependent structures, systems and components, whose safety must be rigorously evaluated through probabilistic safety assessment. During the time between a reactor's emergency shutdown resulting from a mainshock and its subsequent cold shutdown state, some SSCs may experience nonlinear behavior due to the mainshock, but they do not fail. The importance of aftershocks lies in their potential to compound the effects of the mainshock, potentially leading to the failure of these SSCs. In addition, the core damage sequences that were in progress because of the mainshock can be exacerbated by additional failures (e.g., containment functions) due to aftershocks. Therefore, the occurrence of an aftershock during this time frame may affect the NPP safety based on the cumulative damage of both the mainshock and aftershock, which can result in the failure of these SSCs. Analyzing these failures, understanding the accident sequences that they contribute to, understanding how the associated risks can be reduced, and developing other associated insights are the principal tasks of aftershock seismic PSA analysis.

The goal of Task 7.3.2 of METIS is to develop a strategy for consideration of aftershocks in seismic PSA. The activities include survey of state-of-the-art methods and the best practices for consideration of aftershocks in seismic PSA, accounting for the results of:

- WP4 (modelling earthquake sequences for considering aftershocks),
- WP5 (defining a methodology for selecting hazard-consistent aftershock ground motion records to be used to estimate damage-state dependent fragility);
- WP6 (influence of aftershocks on seismic fragility of SSCs);
- Feedback from online METIS Technical Working Meeting "Aftershocks in PSA", February 9th, 14th, 2023.

There are several unique challenges that are associated with an aftershock risk assessment as listed below. Therefore, any strategy needs to consider these challenges.

1. Challenge: Identification of the post-mainshock plant state, status of each of the critical safety functions, and timeframe of importance for aftershock consideration.

2. Challenge: Characterization of the damage state of the plant and that of the SSCs important to safety after the mainshock.

3. Challenge: For use in the aftershock analysis, lack of data to characterize fragilities of SSCs that have suffered partial damage from the mainshock.

4. Challenge: Characterization of the aftershock hazard (conditional probability and/or probabilistic hazard characterization as a function of the "size" of the mainshock).

5. Challenge: For risk insights and estimates of impacts on risk, it is necessary to consider both sequences that do not result in a core damage state after the mainshock analysis but have some damage and accident sequences that result in a specified core damage state but are vulnerable to further damage from the aftershock.

6. Challenge: Understanding the usefulness of modifications made in response to the Fukushima event (e.g., FLEX equipment and offsite resources).

Because of these challenges and some other considerations, Section 2.4 of this report discusses a set of "caveats" that need to be considered in applying the methods herein. Among the most important is the idea that developing a full-scope aftershock seismic PSA may be too complex and resource consuming and unlikely to provide useful safety insights. For example, it may require shake-table tests of partially damaged equipment to determine the probability of further damage in an aftershock. However, despite this caveat, much very useful information can be derived from the methods described in this report.

The first step in a strategy is to identify situations and conditions under which the consideration of aftershocks is important considering the seismicity of a region and the control of mainshock events. Although Section 2 of the report deals with methodology for different elements of an aftershock analysis, the methodology is mostly described from some published papers and not utilized in a

subsequent example. These methods are still evolving and need additional development. Therefore, the current effort is exploratory in nature and, as described below, is focused on practical insights that can be more easily derived and can enhance the plant's safety.

There are several potential objectives of performing an aftershocks seismic PSA analysis, each accompanied by corresponding potential benefits. Besides the objective of developing a seismic core-damage frequency and large-early-release frequency, an important objective could be identifying those SSCs that would play a role in various aftershock accident sequences and identifying measures for each SSC that could be taken in advance to decrease the associated risk. Another important objective could be providing guidance to the NPP operating staff about what actions to take immediately after a seismic mainshock that could substantially decrease the plant's vulnerability to the effects of any subsequent aftershocks. As a general observation, seismic PSA is well suited to these objectives if the analysis is carried out with them specifically in mind and the documentation explains the relevant insights.

Section 1 includes a review of various databases, highlighting past seismic events and the resulting experience feedback and lessons learned, particularly in relation to the effects of aftershocks on power plants' safety (not only on nuclear power plants).

Section 2 deals with the development of the draft strategy for consideration of aftershocks in seismic PSA including changes in usual SPSA components (hazard analysis, fragility assessment, analysis of systems) due to the effects of aftershocks considered.

Sections 3 and 4 contain the results, conclusions, recommendations (including needs for future research in the area of considering aftershocks in SPSA) and acknowledgments.

Section 5 provides a list of references.

The Appendix presents an example application of PSA considering aftershocks to assess their impact on risk.

1. Experience feedback

This chapter endeavors to provide a comprehensive review of various databases, highlighting past seismic events and the resulting experience feedback and lessons learned, particularly in relation to the effects of aftershocks on the safety of power plants (not only on nuclear power plants). Moreover, the report examines experimental data that quantifies the safety of diverse SSCs. Ultimately, the primary objective of this report is to enhance our understanding of the potential impact of aftershocks on NPP safety and to propose effective strategies for addressing this issue within a PSA framework.

1.1. Methodology

The number of existing reports that evaluate the effects of aftershocks on the safety of power plant structures and components is limited. Various data sources, including SQUG, EPRI, SMIRT, HAL, WGIAGE, and NEA, were reviewed, and the findings revealed only a limited number of reports on the assessment of aftershock effects on the safety of power plant structures and components.

The information gathered from the reports is categorized into different sections, including mainshock properties, aftershock properties, structural descriptions, damages caused by the mainshock, facility performance, and damages caused by the aftershock.

1.2. A Review of the Safety Implications of Aftershocks on Power Plants

1.2.1. Investigation of the 1999 Chi Chi Taiwan earthquake /Chi Chi Taiwan/

What follows is drawn from EPRI 1003120:

Mainshock properties

The seismic event of considerable magnitude, registering either 7.3 (ML) or 7.6 (MW), known as the Chi Chi Earthquake, struck at 1:47 AM (local time) on September 21, 1999, with its epicenter situated near the town of Chi Chi in Nantou County. The focal point of the earthquake was approximately 7 km beneath the Earth's surface.

Aftershock properties

Following the main seismic event, a staggering number exceeding 10,000 aftershocks were recorded within a month. Among them, five aftershocks surpassed a magnitude of 6 on the Richter scale. Notably, a 6.7 magnitude aftershock struck on June 11, 2000, exacerbating the existing damage. The epicenters of these aftershocks predominantly clustered on the eastern side (hanging wall) of the Chelungpu Fault.

Structure description

The Taiwan Power Company (Taipower) manages the generation, transmission, and distribution of power for approximately 22 million customers throughout Taiwan. By the end of 1998, Taipower operated 39 hydroelectric plants, 27 thermal plants (utilizing oil, coal, and LNG), and three nuclear generating stations. Their combined installed generating capacity totaled 26,680 MW, with hydroelectric contributing 4,422 MW (16.6%), thermal contributing 17,114 MW (64.1%), and nuclear contributing 5,144 MW (19.3%).

With the rapid economic growth, especially in the industrialized northern region, the demand for electricity has soared. To meet this demand, power generated in the southern and central parts of the island is transmitted to the north via the 345-kV transmission system. Taipower's 345-kV electric

power transmission system features two primary transmission lines that follow similar paths between the northern and southern regions. Both lines converge at the Chungliao switching station.

Damages caused by Mainshock

The Chi Chi Earthquake inflicted severe damage on both the 345-kV and 161-kV systems, primarily due to slope failures in the mountainous regions near the epicenter. While hydroelectric plants in the epicentral zone, anchored on bedrock, largely withstood the quake, substations sustained extensive damage. Fortunately, the three nuclear power stations, located approximately 150 km from the epicenter, remained unscathed. However, the fossil plant near Taichung harbor, about 50 km west of the epicenter, suffered some earthquake-related damage. Notably, the most significant impact on the power system stemmed from the extensive damage to transmission towers and the 345-kV Chungliao switching station.

Facility Performance

Chinshan and Kuosheng Nuclear Generating Stations, located over 100 km from the epicenter, experienced reactor shutdowns post-Chi Chi Earthquake due to damaged transmission infrastructure. Maanshan Nuclear Generating Station, similarly distant, remained operational. No earthquake damage occurred at any plant. Chinshan recorded peak ground accelerations of 0.037g (north-south), 0.034g (east-west), and 0.029g (vertical), while Kuosheng's ground motion was estimated below 0.05g. All Chinshan units were restored within one to four days. Maanshan units stayed online throughout without recorded ground motion data.

Damages caused by Aftershock

There is no investigation on further damages due to aftershocks in the EPRI report.

1.2.2. The Performance of Raceway Systems in Strong-Motion Earthquakes: The Chile Earthquake /Raceway Systems/

What follows is drawn from EPRI NP-7150-D:

Mainshock properties

The Chile earthquake struck on March 3, 1985, at 7:47 P.M. (local time), with a magnitude of 7.8, originating 15 miles offshore from Chile's central region, including the capital city of Santiago, home to around 6 million people. The seismic event and its aftershocks resulted in 180 fatalities, over 2,500 serious injuries, and the destruction of more than 45,000 homes, causing nearly $2 billion (U.S.) in direct damages. Lasting approximately 2 minutes, with strong ground motion persisting for up to 40 seconds, the earthquake generated Modified Mercalli intensities reaching up to IX along the coast and VII to VIII across a significant coastal and inland area.

Aftershock properties

Following the main earthquake, a significant aftershock sequence ensued, including a magnitude 7.0 aftershock just one hour later and a 7.2 magnitude event on April 9 which occurred 15 miles west of the site.
The affected region hosts numerous power and industrial facilities, many of which were promptly assessed post-earthquake. Overall, these facilities demonstrated swift recovery, successfully repairing significant damage and resuming production. Seismic damage to well-engineered systems and structures was minimal compared to the moderate to heavy damage sustained by surrounding residential and commercial areas. Anchored equipment, piping, and other power plant components generally withstood the seismic activity admirably.
Subsequently, inspection reports detailing the performance of various facilities are reviewed.

Structure description (Renea Power Plant)

The Renca Power Plant, situated in Santiago approximately 85 miles east of the earthquake's epicenter, occupies an area heavily affected by damage to adobe and masonry structures. Owned by

Chilectra Generacion and completed in 1962, the plant features two 50 MW coal-fired rod-hung boiler units and two turbine generators mounted on reinforced concrete pedestals. Both the turbine and boiler structures are reinforced with braced steel frames.

Adjacent to the turbine building are two sizable timber cooling towers and a 110 kV switchyard. Other structures on-site include a single-story concrete-frame building housing the Chilectra Dispatch Center, a coal conveyor system delivering coal to the turbine building's upper level, and a water treatment facility. The plant sits on a flat site with deep alluvial soil. Internal infrastructure comprises 18-inch-wide ladder-type cable trays supported by rod-hung trapezes, with typical spans ranging from 8 to 10 feet between supports.

Damages caused by Mainshock

Seismic damage at the Renea Power Plant included bent seismic restraints for the suspended boilers, leaky tubes in the Unit 1 boiler, failed anchor bolts on large horizontal tanks, and broken bolts at the bases of three transformers. Despite the severity of the quake, two unanchored motor control centers only slid up to 12 inches, halted from overturning by conduit connections at the base. Remarkably, the cable trays remained undamaged by both the earthquake and its subsequent aftershocks.

Facility Performance

Neither unit was in operation during the earthquake, with Unit 1 undergoing maintenance. Unit 2, after a cursory inspection within 5 hours of the seismic event, was swiftly brought online and operated through subsequent aftershocks.

Damages caused by Aftershock

There is no investigation on further damages due to aftershocks in the EPRI report.

Structure description (Rapel Hydroelectric Plant)

The Rapel Hydroelectric Plant, positioned 65 miles southeast of the main earthquake epicenter, lies in an area heavily affected by landslides and rockfalls. The facility boasts a substantial concrete arch dam housing five generators, each with a capacity of 75 MW. The dam stands at an impressive 345 feet in height and spans 1,150 feet in length, nestled within a natural river gorge on rugged terrain. Adjacent to the dam, the switchyard and control building perch atop an adjacent hill. The generators, commissioned between 1968 and 1970, have been pivotal to the plant's operation.

Damages caused by Mainshock

None of the five turbines were operational during the earthquake. Post-earthquake inspection revealed minor damage to the dam. The emergency diesel was promptly activated and ran for 24 hours until three units were restored to service. However, two other units faced foundation movement issues and remained offline. The delay in startup primarily stemmed from damage to the 220 kV switchyard.

Minor damage was observed in the control building equipment, while no harm was reported to cable trays or conduit.

Damages caused by Aftershock

In the days following the earthquake, further examination revealed additional damage to the dam. The direct cost of this damage was estimated at $20 million, with an additional loss of approximately $11 million attributed to the unavailability of Units 3 and 5. **Interestingly, little to none of the damage was attributed to aftershocks.**

1.2.3. The Performance of Raceway Systems in Strong-Motion Earthquakes: The Mexico Earthquake /Raceway Systems/

What follows is drawn from EPRI NP-7150-D:

Mainshock properties

The Mexico earthquake struck on September 19, 1985, at 7:17 A.M. (local time), registering a magnitude of 8.1. Its epicenter was located roughly 25 miles northwest of the industrial town of Lazaro Cardenas. The seismic event reverberated across southwestern Mexico and was felt as far away as Galveston, Texas.

Aftershock properties

On September 20, at 7:34 P.M., a 7.5 magnitude aftershock hit approximately 70 miles southwest of the mainshock epicenter.

Structure description

Two major hydroelectric plants are situated in the epicentral area. The 1000 MW El Infiernillo plant is approximately 40 miles from the mainshock, while the 300 MW La Villita plant is a mere 25 miles from the epicenter.

Damages caused by Mainshock

Damage to the dams was confined to superficial harm at the dam crests. At El Infiernillo, an oil leak transpired in a high-voltage transformer within the switchyard, while at La Villita, only a few ceiling panels fell in the control room.

Damages caused by Aftershock

There is no investigation on further damages due to aftershocks in the EPRI report.

1.2.4. The Performance of Raceway Systems in Strong-Motion Earthquakes: the Adak, Alaska Earthquake /Raceway Systems/

What follows is drawn from EPRI NP-7150-D:

Mainshock properties

On May 7, 1986, at 1:47 P.M. (local time), a magnitude 7.7 earthquake struck southeast of the Andreanof Islands chain, approximately 90 miles southeast of Adak, Alaska. Preceding the main event, three foreshocks of magnitudes 4.5, 6.0, and 5.0 occurred within the 3 hours leading up to it.

Based on personal interviews and observations, the intensity of shaking is estimated to have ranged between V and VII on the Modified Mercalli Intensity Scale, varying with the location on the island. Preliminary estimates suggest a range of Peak Ground Accelerations (PGAs) between 0.15g to 0.25g, based on observed damage.

Aftershock properties

Following the main earthquake, two significant aftershocks of magnitudes 6.2 and 6.5 occurred on May 8 and May 17, respectively. Although a tsunami warning was issued, no significant wave heights were generated. However, reports indicated a drop in water level by several feet in Sweeper Cove.

Structure description

On Adak Island, existing structures comprise timber-frame, reinforced masonry, precast reinforced concrete, and various steel constructions. Most buildings are limited to three stories or fewer in height. The island infrastructure includes diesel generator power plants, steam plants, electrical substations, and numerous facilities equipped with computer equipment and emergency power facilities.

Damages caused by Mainshock

The power plant sustained only minor damage from the earthquake, with no reported harm to cable raceways or cables. The building experienced only minor cracking in the floor slab.

Damages caused by Aftershock

Approximately one week after the mainshock, damage was discovered on the outboard bearing of one of the diesel generators. **The damage was attributed to a misalignment, likely caused by the earthquake or one of its aftershocks.**

1.2.5. Earthquake of October 9, 1995: Effects at the Manzanillo Power Plant /Manzanillo/

What follows is drawn from EPRI TR-108478:

Mainshock properties

A magnitude 7.6 earthquake in the subduction zone off the Pacific Coast of Mexico inflicted serious damage to the Manzanillo Power Plant, one of the largest thermoelectric generating plants in the nation's power system.

Aftershock properties

Throughout the remainder of Monday, October 9, the Manzanillo free-field instrument detected a total of 16 aftershocks, with recorded peak ground accelerations ranging from 0.005 to 0.03g. This sequence of smaller aftershocks persisted into Tuesday and Wednesday. Notably, a magnitude 5.0 aftershock occurring shortly after midnight on Tuesday, October 10, registered a peak ground acceleration of 0.15g.

On Thursday, October 12, a significant aftershock measuring magnitude 5.6 struck at 10:53 a.m. The free-field instrument recorded a peak ground acceleration of 0.15g. The intensity of the October 12 aftershock alone warranted detailed examination, representing an exemplary scenario for design basis earthquakes, particularly relevant for nuclear power plants in the eastern United States.

Structure description

The Manzanillo Power Plant encountered ground shaking of unprecedented severity, ranking among the most intense ever recorded beneath a large modern power facility. Horizontal motions measuring approximately 0.40g peak ground acceleration were documented in the plant's substation, with records captured in both horizontal directions. Additionally, motions of buildings and equipment were also documented.

Damages caused by Mainshock

The strong motion endured for approximately 30 seconds, characterized by a broad-band frequency content, resulting in significant damage to the 400-kilovolt substation switchyard due to the collapse of ceramic components. Additionally, the plant's buried concrete cooling water intake system structures suffered damage due to localized liquefaction. While this type of damage has been observed in past earthquake investigations, it was not surprising given the severe level of motion.

Remarkably, most other systems within the modern power plant withstood the earthquake admirably, and the plant resumed operation without issues once the generating units were brought back online. The performance of the Manzanillo plant serves as another testament to the general durability of power generating stations in withstanding strong ground motion.

Facility Performance

The Manzanillo plant, being the largest and most modern, likely endured some of the most severe shaking based on its ground motion record. While it didn't suffer widespread damage, it fared worse than all but one of the earthquake-affected power plants in the EPRI database. The only plant with more significant damage was the U.S. Navy steam plant serving Guam during the 1993 magnitude 8.0 earthquake.

Similar to Manzanillo, this older oil-fired plant experienced liquefaction damage at its saltwater intake structure, leading to the collapse of buried concrete piping serving the plant condensers. Repairing the liquefaction damage kept the largest unit of the Navy plant offline for three months following the earthquake.

Damages caused by Aftershock

The magnitude 5.6 aftershock had negligible effects on the two Manzanillo plants. Since all generating units were already shut down and undergoing repairs due to damage sustained from the mainshock three days prior, the aftershock had no consequential impact.

1.2.6. The January 17, 1994, Northridge Earthquake: Effects on Electric Power and Selected Industrial Facilities /Northridge Earthquake/

What follows is drawn from EPRI TR-106635:

Mainshock properties

On Monday, January 14, 1994, at 4:31 AM (PST), a moment magnitude 6.7 (MW) earthquake struck the Northridge area of metropolitan Los Angeles, California. It stood out as one of the most significant earthquakes to hit a densely populated area in the United States since the 1906 San Francisco Earthquake. The 1994 Northridge Earthquake incurred approximately $20 billion in damages and is estimated to have resulted in one of the highest amounts of insured losses due to a natural disaster in U.S. history.

Aftershock properties

Aftershock activity following the Northridge Earthquake was notable, with 13 aftershocks registering magnitudes equal to or greater than 4.0 between January 18 and 28. Despite the heightened level of aftershock activity, the decay in aftershock frequency aligned with patterns observed in other significant earthquakes in California.

Structure description

Situated closest to the epicenter, the Valley Generating Station comprises four thermal generating plants. Unit 1 has a rating of 95,000 kW, while unit 2 is rated at 99,000 kW. Both units were commissioned in 1954 and were subsequently placed in mothball status in 1994 after many years of service. Units 3 and 4, with ratings of 163,000 kW and 160,000 kW respectively, had not been operational since November 1993.

Damages caused by Mainshock

The facility incurred minor damage, including cracks in steel struts, a twisted wide flange support, distorted exhaust duct insulation panels, damaged piping supports and insulation, and inoperable

combustion air instruments. Additionally, superficial damage was observed on various building elements. However, these issues did not hinder the plant's start-up process.

Regarding protective relays, it is typically challenging to distinguish instances where relays change state due to contact chatter. Protective relays are designed to trip during electrical disturbances, such as grid loss, and may also be susceptible to vibration-induced chatter based on shake-table test data for specific models. Fortunately, all relays remained undamaged and fully functional following the earthquake.

Damage sustained during the mainshock included:

- 230 kV apparatus, such as the reactor box, circuit breaker with oil leak, and potential transformer (PT).
- Transformers, with issues noted in bushings and bus connections, radiator oil pipe leaks, oil conservator leaks, and surge arresters.

Furthermore, at building 40, which housed the main boilers and chillers, significant damage was observed. The main 14-inch diameter supply line to the main chillers sheared off approximately 3 inches below the flanges where the vertical run of the pipe entered the ground. Additionally, the natural gas line for the main boilers featured an in-line seismic shut-off valve that continued to trip during strong aftershocks. To mitigate frequent shutdowns of the boilers, operators bypassed the seismic shut-off valve.

Facility Performance

At the time of the earthquake, which occurred at 4:31 a.m. (PST), Unit 3 was on reserve shutdown status, while Unit 4 was unavailable due to a planned outage. As a result of the grid blackout, the plant immediately lost power. Units on reserve shutdown are in a cold condition but remain available to generate power. However, unlike units in hot shutdown, it can take several hours to restart auxiliary systems, prepare the boiler for operations, and generate steam.

Damages caused by Aftershock

During the magnitude 5.1 aftershock on January 19, two days after the mainshock, the plant was in operation. **No significant physical damage was observed; however, Unit 4 tripped offline due to relay actuation, indicating phase-to-phase and phase-to-ground faults.**

Receiving stations S and T receive 230 kV transmission from RS-E and RS-U, respectively, distributing at 34.5 kV to the Nuys and Woodland Hills areas, respectively. Following an aftershock several days after the mainshock, a transformer fire occurred at RS-S. The probable cause of the fire appeared to be a misaligned bushing.

1.2.7. Investigation of the 1999 Kocaeli Turkey Earthquake /Turkey Earthquake/

What follows is drawn from EPRI 1003119:

Mainshock properties

On August 17, 1999, a magnitude 7.4 (MW) earthquake devastated the city of Izmit in the province of Kocaeli, located in western Turkey. The catastrophic event resulted in the collapse of over 20,000 buildings, claiming the lives of 17,000 individuals and injuring 44,000 others. The earthquake also inflicted an estimated economic loss of US $16 billion.

Aftershock properties

At 8:54 AM, a powerful aftershock struck, leading to the complete de-energization of the entire grid once more. Consequently, the step-by-step restoration process had to be initiated anew.

Structure description

The Ambarli Fuel Oil Power Plant, situated approximately 130 km west of Istanbul, consists of five units with a total generating capacity of 630 MW. Constructed over several years from 1967 to 1971, the plant experienced a peak horizontal ground acceleration of 0.25g as recorded by the Kandilli station at the Ambarli site. Loss of offsite power led to the plant tripping offline. However, six days after the earthquake, all units were operational under controlled conditions.

Damages caused by Mainshock

Following the earthquake, no significant damage was reported to the boilers, turbine generators, or their support structures at the Ambarli Fuel Oil Power Plant. However, minor damage and anomalies were observed, including:

1. Damage to the spring supports of Units 4 and 5 condensers.

2. Higher vibration of the Unit 4 turbine generator.

3. Stretching of two 1-3/4-inch diameter anchor bolts of the Units 4 and 5 boiler structure columns by 1/4 inch.

4. Pounding damage to the floor slab at the operating deck of Units 4 and 5.

5. Damage to elevators in Units 4 and 5, including a snapped cable, damage to the braking system of the counterweight, and deformation of the counterweight guide rails.

6. Damage to the brick cylindrical extension at the top of the reinforced concrete stack of Units 4 and 5, designed to protect personnel during inspections and to release the plume.

Facility Performance

By early afternoon on the day of the earthquake, local grids were energized, providing electricity at 34.5 kV. Distribution service was largely restored by the evening of August 17th, except for areas with damaged circuits. It is worth noting that the electrical transmission system in Turkey was undergoing significant expansion at the time of the earthquake. Consequently, the availability of new equipment and materials greatly facilitated the restoration efforts.

Damages caused by Aftershock

Around noon on the day of the earthquake, during an aftershock, the brick enclosure collapsed, resulting in damage to gas isolation equipment housed in the building located below the enclosure.

1.2.8. SMART 2013: Experimental and numerical assessment of the dynamic behavior by shaking table tests of an asymmetrical reinforced concrete structure subjected to high intensity ground motions /SMART 2013/

As part of a large research program launched and funded by the French Atomic Energy and Sustainable Energies Commission (CEA) and Electricité De France (EDF), partially supported by the International Atomic Energy Agency (IAEA) and entitled "Seismic design and best-estimate Methods Assessment for Reinforced concrete buildings subjected to Torsion and nonlinear effect (SMART)", a series of shaking table tests on a ¼-scale 3-story reinforced concrete model characterized by a strong asymmetry was carried out in July 2013.

Mainshock properties

The seismic loading was composed of three test sequences having different peak ground accelerations (PGA): the design level signal (PGA equal to 0.2 g), the Northridge mainshock signal (PGA equal to 1.78 g) and a Northridge aftershock (PGA equal to 0.33 g).

Damages caused by Aftershock

The fact that no additional damage was monitored during this seismic sequence was pointed out only by the experimental measurements but also by the numerical outputs, leading to show that this aftershock signal did not induce any further damage.

1.2.9. Preliminary Findings and Lessons Learned from the 16 July 2007 Earthquake at Kashiwazaki-Kariwa NPP /Earthquake at Kashiwazaki-Kariwa NPP/, /Niigata-Chuetsu Oki, Japan/

What follows is drawn from IAEA Report on Kashiwazaki-Kariwa Nuclear Plant:

Mainshock properties

The M6.6 mainshock of the Niigata Chuetsu Oki (offshore) earthquake occurred at 10:13 a.m. local time on July 16, 2007. The mainshock had an estimated focal depth of 10 km (USGS, 2007) and struck in the Japan Sea offshore Kariwa.

The JMA (Japan Meteorological Agency) seismic intensity was 6+ (IX in MMI) in Kariwa-cho, Kashiwazaki city, and Nagaoka city in Niigata prefecture, and Ohzunamachi in Nagano prefecture /Niigata-Chuetsu Oki, Japan/.

Aftershock properties

The Niigata Chuetsu Oki earthquake was followed by a sequence of aftershocks. The largest aftershock as of 10:00 on July 17, was a M5.8 (preliminary) earthquake that occurred at 15:37 on July 16, with maximum seismic intensity 6 Lower.

Structure description

Kashiwazaki-Kariwa nuclear power plant is the biggest nuclear power plant site in the world. It is operated by Tokyo Electric Power Company (TEPCO). The site has seven units with a total of 7965 MW net installed capacity. Five reactors are of BWR type with a net installed capacity of 1067 MW each. Two reactors are of ABWR type with 1315 MW net installed capacity each. The five BWR units entered commercial operation between 1985 and 1994 and the two ABWRs in 1996 and 1997 respectively.

Facility Performance

At the time of the earthquake, four reactors were in operation: Units 2, 3 and 4 (BWRs) and Unit 7 (ABWR). Unit 2 was in start-up condition but was not connected to the grid. The other three reactors were in shutdown conditions for planned outages: Units 1 and 5 (BWRs) and Unit 6 (ABWR).

Although the Niigataken Chuetsu-Oki earthquake on 16 July 2007 significantly exceeded the level of the seismic input taken into account in the design of the plant, the installation behaved in a safe manner, during and after the earthquake. In particular, the automatic shutdown of the reactors of Units 3, 4 and 7, which were operating at full power, and of the reactor of Unit 2, which was in the start-up state, were performed successfully.

Damages caused by Mainshock

The earthquake caused automatic shutdown of the operating reactors, a fire in the in-house electrical transformer of Unit 3, release of a very limited amount of radioactive material to the sea and the air and damage to non-nuclear structures, systems and components of the plant as well as to outdoor facilities, as reported by TEPCO on their web page.

Preliminary data indicated that the design basis ground motion for the plant might have been

exceeded, with possible significant effects on the behavior of the plant SSCs.

Damages caused by Aftershock

IAEA report does not include any information on additional damages caused by aftershocks.

1.2.10. The performance examination of Onagawa nuclear power station's SSCs following the great east Japanese earthquake and tsunami /Tohoku earthquake and tsunami, Japan/

What follows is drawn from IAEA issues Report on Onagawa nuclear power station:

Mainshock properties

The 2011 Off the Pacific Coast of Tohoku Earthquake struck at 05:46 UTC (14:46 JST) on March 11, 2011, with a magnitude (Mw) of 9.0. This powerful earthquake triggered extreme vibratory ground motion and a devastating tsunami. Given the widespread disaster it caused along the east coast of Japan, the earthquake is commonly referred to as the Great East Japan Earthquake (GEJE).

Aftershock properties

The mainshock of the GEJE was preceded by a strong motion foreshock and followed by numerous aftershocks that extended over a prolonged period. Seismographs at the Onagawa Nuclear Power Station recorded some of these aftershocks. Additionally, the earthquake generated large tsunamis that overtopped a limited area of the Nuclear Power Station.

Structure description

The Onagawa Nuclear Power Station comprises three boiling water reactors (units), with Unit 1 in operation for the past twenty-eight years since its commercial operation commenced in June 1984. Unit 2 began commercial operation in July 1995, followed by Unit 3 in January 2002. Collectively, the three units have a combined electric generation capacity of 2,174 megawatts.

Located on the eastern coast of Japan facing the Pacific Ocean, the Onagawa Nuclear Power Station was the closest nuclear power station to the epicenter of the enormous M9.0 GEJE. Due to its proximity to the earthquake source, the plant experienced unprecedented levels of ground motion, representing the strongest shaking ever encountered by any nuclear power plant from an earthquake. Despite this, the plant shut down safely.

Damages caused by Mainshock

The Structures Team noted that safety-related building systems (Class S) performed well across all three units of the Onagawa NPS, while some cracking and deformation were observed in turbine buildings (Class B). Thankfully, no loss of coolant accidents occurred, and emergency core cooling systems were not needed. However, turbines in Units 2 and 3 sustained damage.

During the March 11 earthquake, main transformers for all three units, startup transformers for Units 1 & 2, and house & auxiliary boiler transformers for Unit 2, experienced oil pressure relief valve actuations and over-pressure alarms due to insulating oil sloshing in the transformer tanks.

The Systems Team concluded that safety systems functioned successfully, with non-safety and lower-class seismic systems shutting down the plant effectively. The tsunami caused more damage than the earthquake, particularly affecting Unit 2's shutdown cooling systems. The most significant earthquake damage was to turbines in Units 2 and 3, designed to lower seismic standards.

Damages caused by Aftershock

At the time of the biggest aftershock on April 7, main & house transformers for all three units, startup, auxiliary boiler & exciter transformers for Unit 2 experienced the same

events as above. Activation of pressure switches in oil-insulated transformers due to sloshing is a common earthquake effect.

1.3. Conclusion

Table 1 summarizes the available reports regarding the effects of aftershocks. As previously noted, there is limited report on the impact of aftershocks on power plants and their SSCs. **However, existing reports show that aftershocks generally do not directly cause additional damage to the main reactor structures. Instead, aftershocks tend to cause further damage to subsystems that were already weakened by the mainshock, particularly those associated with masonry structures or subsystems that were not properly aligned as a result of the mainshock.**

In some instances, damaged subsystems cause delays in bringing the power plant back on-line after a mainshock-induced safe shutdown.

Power plant	Earthquake	Mainshock properties	Aftershock properties	Time between MS and AS	Damages to parts of power plant system due to MS	Damage reported during or after AS	Main reason of AS damages
Taipower (3 NPP, 3 Hydro PP and 2 Fossil PP)	Chi Chi Taiwan, 1999	Magnitude 7.3 (M_L) or 7.6 (M_W) at 1:47 AM (local time) on September 21	10,000 aftershocks within a month/ Five aftershocks magnitude≥ 6 Richter	140 days until the biggest AS (M=6.7)	Severe damage to the transmission towers and the 345-kV Chungliao switching station	-	-
Renca (Fossil PP)	Chile, 1985	Magnitude 7.8 at 7:47 P.M. (local time) on March 3	A magnitude 7.0 aftershock one hour after the mainshock and a 7.2 magnitude event on April 9	1 hour until the first big AS (M=7) and 36 days until the second big one	Bent seismic restraints for the suspended boilers, leaky tubes in the Unit 1 boiler, failed anchor bolts on large horizontal tanks, and broken bolts at the bases of three transformers. Two unanchored motor control centers slid up to 12 inches but were prevented from overturning by conduit connections at the base	-	-
Rapel (Hydro PP)	Chile, 1985	Magnitude 7.8 at 7:47 P.M. (local time) on March 3	A magnitude 7.0 aftershock one hour after the mainshock and a 7.2 magnitude event on April 9	1 hour until the first large AS (M=7) and 36 days until the second one	Damage in the 220 kV switchyard	-	-
El Infiernillo and La Villita (Hydro PPs)	Mexico, 1985	Magnitude 8.1 at 7:17 A.M. (local time) on September 19	A magnitude 7.5 aftershock	About 36 hours	An oil leak in a high-voltage transformer in the switchyard at El Infiernillo, and falling a few ceiling panels in the control room at La Villita	-	-
Diesel generator PPs	Adak, Alaska, 1986	Magnitude 7.7 at 1:47 P.M. (local time) on May 7	Two large ASs of magnitudes 6.2 and 6.5 on May 8 and May 17, respectively	1 day until the first large AS and 10 days until the second one	Only minor cracking in the building floor slab	-	-
Manzanillo (thermoelectric generating plants)	The Pacific Coast of Mexico, 1995	Magnitude 7.6 on October 9	Two large ASs of magnitudes 5.0 and 5.6 ASs on October 10 and October 12, respectively produced peak ground acceleration of 0.15g	Less than 24 hours until the first large AS (M=5) and about 4 days until the second one	Serious damage to the 400-kV substation switchyard due to collapse of ceramic components, and to the plant's buried concrete cooling water intake system structures due to localized liquefaction	-	-

Power plant	Earthquake	Mainshock properties	Aftershock properties	Time between MS and AS	Damages to parts of power plant system due to MS	Damage reported during or after AS	Main reason of AS damages
4 thermal generating plants	Northridge, 1994	Magnitude 6.7 (Mw) at 4:31 A.M. (PST) on January 14	There were 13 aftershocks of magnitude greater than or equal to 4.0 between January 18 and 28.	4 to 14 days	230 kV apparatus (reactor box, circuit breaker oil leak, PT) and transformers (bushings and bus connections, radiator oil pipe leaks, oil conservator leaks, surge arresters)	No significant physical damage was observed; however, unit 4 tripped off-line due to relay actuation. A transformer fire occurred at RS-S following an AS, several days after the MS.	The probable cause of the fire appeared to be due to a misaligned bushing.
Ambarli (Fuel Oil PP)	Kocaeli Turkey, 1999	Magnitude 7.4 (Mw) at 3:02 A.M. (local time) on August 17	Over 2,400 aftershocks, but none over the magnitude of 6	About 6 hours	Damage to elevators, spring supports, stretch of anchor bolts diameter, brick enclosure, etc.	A brick enclosure collapsed	Previous damages by mainshock
a ¼-scale 3-story reinforced concrete model	a series of shaking table tests	Magnitude 6.7 (Mw), the Northridge mainshock signal (PGA equal to 1.78 g)	A Northridge aftershock (PGA equal to 0.33 g), magnitude 5.2	-	Cracking in a shear wall, crushing of the concrete at the junction between a shear wall and the foundation	-	-
Kashiwazaki-Kariwa (NPP)	Niigataken Chuetsu-Oki, Japan, 2007	Magnitude 6.6 at 10:13 A.M. (local time) on July 16	Magnitude 5.8 at 15:37 P.M. (local time) on July 16	About 5 hours	A fire in the in-house electrical transformer of Unit 3, release of a very limited amount of radioactive material to the sea and the air and damage to non-nuclear SSCs of the plant as well as to outdoor facilities	-	-

Table 1: Summary of reports regarding the effects of aftershock

2. Strategy for Consideration of Aftershocks in Seismic PSA

Aftershocks are repeated shocks that occur after the main earthquake and result from the redistribution of stresses in the earthquake source. From a physical point of view, aftershocks do not differ from the mainshocks, though their causes of occurrence somewhat differ.

Aftershocks are understood as clusters of seismic events in which the strongest event is at the beginning in the time period (mainshock). To assess seismic hazards, earthquake catalogues with excluded aftershocks ("declustering") are commonly used. However, aftershocks themselves are also significant since they affect objects that may already be damaged by the impact of the main earthquake, especially weak structures, without proper seismic design.

Working first to understand the safety features and functions of the plant that are vulnerable to damage from an aftershock may provide some insights into the aspects of the aftershock hazard and plant performance that are most important to understand better, on a site-specific basis. The period that is important to nuclear safety from the aftershock perspective is shortly after the mainshock, when the aftershock can exacerbate an ongoing accident and when there is insufficient time to take measures to compensate for a weakened plant. Once the plant is examined and made safe for the operating conditions whatever they may be, any aftershock is more like a new seismic event. Also, the offsite FLEX-type capability could play an important role.

In order to determine the strategy for consideration of aftershocks in SPSA, Internet resources were searched (Web-based ADAMS, SpringerLink, etc.) to find approaches that have been already developed to model aftershocks in SPSA. As a result, a strategy for consideration of aftershocks in SPSA that is based on the report /JNES/ is proposed. The report was published in the summary report NEA/CSNI/R(2007)14 from the "Specialists Meeting on Seismic Probabilistic Safety Assessment (SPSA) of Nuclear Facilities", held in Jeju, Korea, 6-8 November 2006. It should be mentioned that this issue regarding safety significance of aftershocks in seismic PSA was not considered to be crucially important by the experts who participated in the OECD/NEA workshop and no specific recommendation was made regarding this issue (where other weaknesses or recommendations were addressed, e.g. probabilistic seismic hazard analysis, human reliability and treatment of correlations).

The methodology for SPSA considering strong aftershocks, addressed in this Strategy includes the following:

1) Seismic hazard analysis of aftershocks: aftershock activity can be predicted by combining the estimate of the number of aftershocks after the mainshock and the frequency of aftershocks of certain magnitude. Seismic motions caused by the aftershocks are estimated from the attenuation equation or fault model, taking into account the spatial distribution of aftershocks in the source area (see section 2.1).

2) Seismic fragility assessment: the fragility of SSCs can be estimated by considering seismic vibrations caused by the mainshock and aftershocks that can occur within a short period of time (see section 2.2). This concept needs further evaluation.

3) Analysis of systems: reliability analysis of NPP systems taking into account additional impacts (failures) caused by aftershocks while the reactor plant is in cold shutdown state after the emergency shutdown resulting from the mainshock (see section 2.3).

The method for consideration of aftershocks in SPSA is schematized in Figure 1. As shown in the figure, the seismic PSA methodology for aftershocks consists of seismic hazard analysis, SSC fragility evaluation and system analysis. This procedure is basically the same as the SPSA procedure for mainshocks. The time frame over which aftershocks are to be considered and the number of aftershocks are important and need to be discussed. In our view, the analysis does not need to

consider multiple aftershocks.

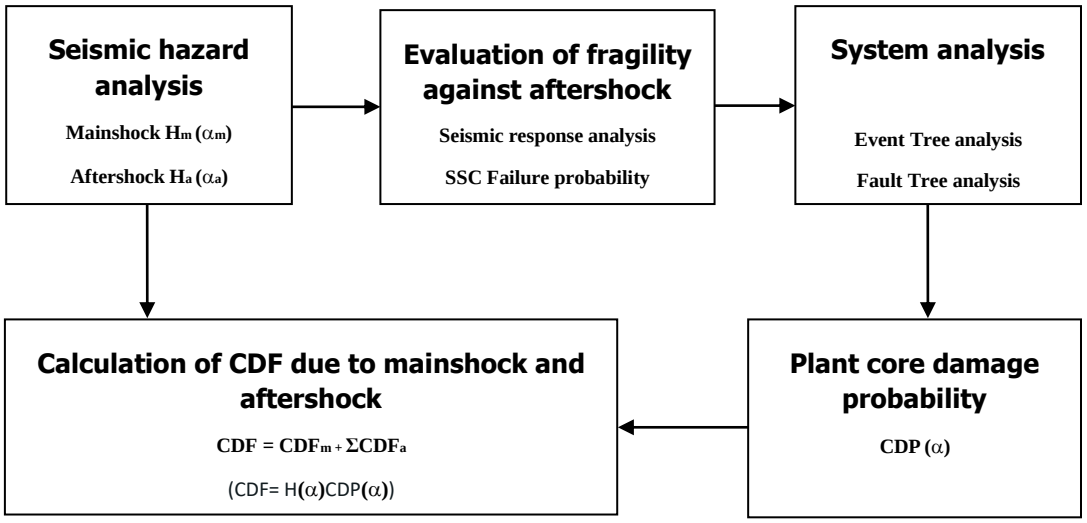

Figure 1: Overview strategy for consideration of aftershocks in seismic PSA

The total risk contribution is quantified to use a simplified formula.

$$CDF = \sum_{i=1}^{n} [Hm_i . CDPm_i] + \sum_{i=1}^{n} \left\{ (1 - CDPm_i) \sum_{j=1}^{k} [Ha_j CDPa_j] \right\}$$

where:
n - hazard intervals used to calculate CDF;
k - number of aftershocks.

However, since SPSA for aftershocks should take into account damage of SSCs from the mainshock in the evaluation of SSC fragility and system analysis, such assessment will be more complex than in the case of SPSA that considers only the mainshock. Thus, when the effect of aftershocks cannot be ignored (as compared to the impact of the mainshock), "full aftershock seismic PSA" (Levels 1, 2) can be performed. Figure 2 schematically shows how the impact of aftershocks on seismic hazard or fragility is taken into account in seismic PSA. It is important that the sequences that result in core damage states after the mainshock are also considered to see if the risk is exacerbated because of the aftershocks. This was an important question after the Fukushima accident.

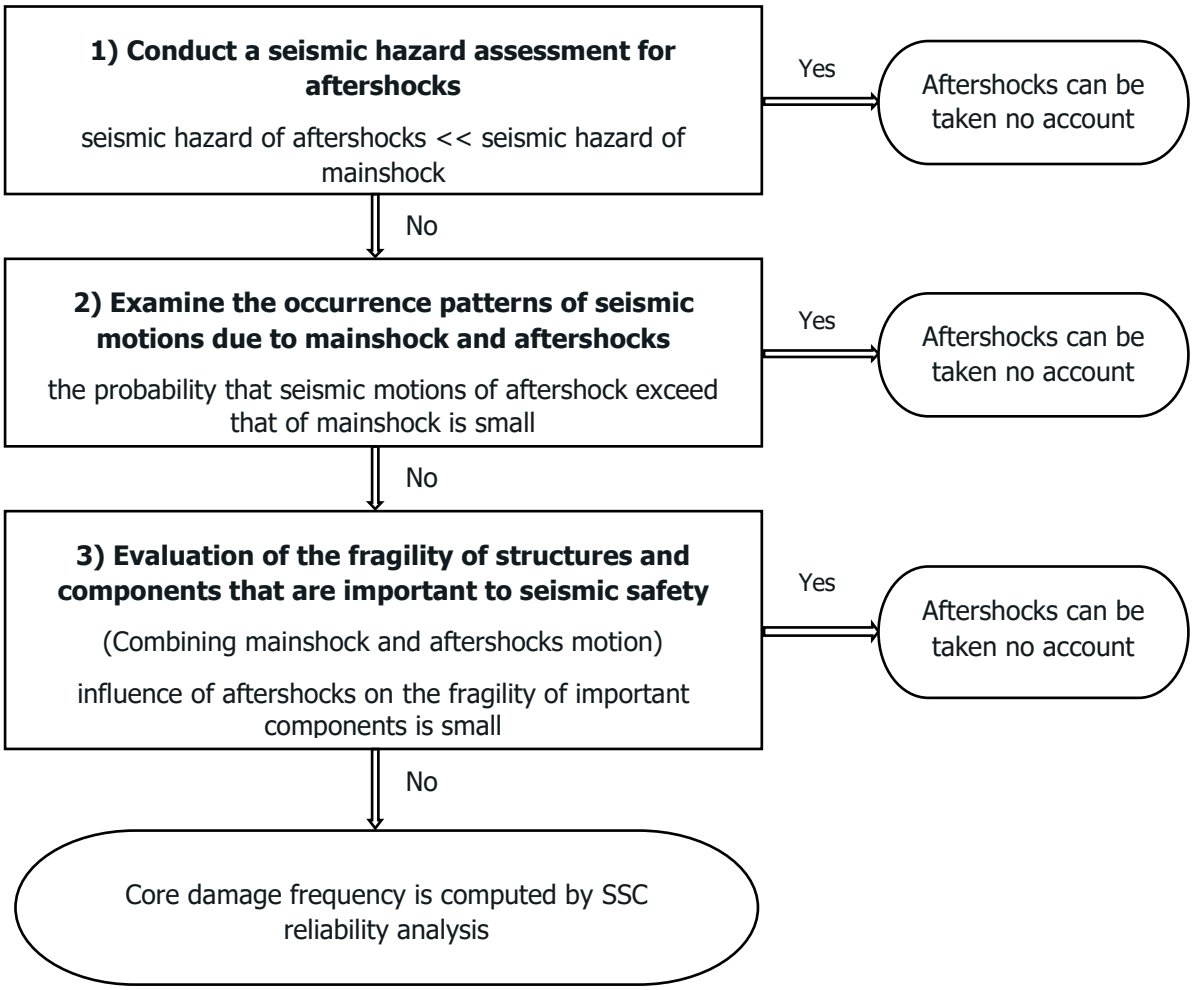

Figure 2: Influence of aftershocks on seismic hazards and fragility evaluation in seismic PSA (screening)

2.1. Analysis of Aftershock Seismic Hazard

To assess the seismic hazard of aftershocks, a model should be developed for stochastic prediction of aftershock activity. The following in this chapter is an excerpt from METIS Deliverable 4.4: New PSHA methodologies, Section IV: Classical PSHA with Aftershocks.

This chapter describes the theory and methods for calculating aftershocks based on statistical aftershock productivity parameters and how they may be adopted for the generation of stochastic event sequences containing aftershocks (for a single mainshock or for many mainshocks).

2.1.1. Aftershock productivity

Aftershocks are assumed to follow a truncated Gutenberg-Richter distribution /Felzer, Abercrombie, and Ekstrom 2004/, where the total number of earthquakes N above some magnitude M is quantified as

$$N = 10^{a-bM}. \qquad (1)$$

N is a function of the mainshock magnitude M_{main}:

$$N(M_{main}) = c10^{\alpha M_{main}} \qquad (2)$$

where α = 1.0 and $c \approx 0.02$, based on the global analysis by /Felzer, Abercrombie, and Ekstrom

2004/. c is a scalar aftershock productivity parameter, while α controls the scaling with mainshock magnitude.

The *a*, *b*, and M_{max} parameters for the truncated Gutenberg-Richter distribution must be defined as well. The *b* parameter is calibrated based on observed seismicity, jointly with *c*. M_{max} is more challenging to determine from seismicity data, as it is necessarily tied to the declustering process (during the construction of the seismic catalogue used in the development of the mainshock PSHA model) and explicit choices about whether a smaller event shortly before a larger event is a foreshock or whether it is a mainshock with a larger aftershock. To be clear, this classification does not come from the data but is an explicit and somewhat semantic decision made by the modeler. Nonetheless, there are two obvious choices for the aftershock M_{max} parameter: it may be the regional mainshock M_{max} (in which case it will be as large or larger than any given mainshock), or it may be related to the mainshock magnitude, for example equal to that magnitude (or perhaps smaller by a delta, as following Båth's law). The *a* parameter is calculated algebraically by relating Eq. 1 and Eq. 2.

2.1.2. Estimation of aftershock productivity parameters

The first step in the process of calculating the aftershock occurrence rates is to estimate the aftershock productivity parameters. This step should come after the seismic catalogue has been declustered, and requires the association of aftershocks removed in the declustering process with the causative mainshock. This association is not always part of the declustering procedure, depending on the methods used, so additional post-declustering analysis of the mainshock and aftershock catalogues may be necessary.

We use a nonlinear Monte Carlo inversion for the aftershock productivity parameters *b* and *c*, defined in Eq. 1 and Eq. 2, respectively.

First ranges are defined for *b* and *c*, and then some large number of samples is drawn from uniform distributions based on those ranges. Each sample value of *b* is paired with a sample value of *c*.

For each (*b, c*) pair, we iterate over all of the mainshock-aftershock clusters from the observed seismic catalogue and calculate the likelihood of observing the empirical magnitude-frequency distribution of the cluster given the truncated Gutenberg-Richter distribution for the values of M_{main}, b, and c considering the year of the mainshock and the catalogue completeness for that year. The total likelihood of each (*b, c*) pair is the geometric mean of the (*b, c*) pair likelihoods for each mainshock cluster.

This method produces a distribution of likelihoods, so that the single best (most likely) estimate for (*b, c*) can be chosen, or numerous values can be sampled proportional to their likelihood (i.e., Bayesian sampling) in order to incorporate epistemic uncertainties into the aftershock production rates.

Currently, the aftershock productivity parameter estimation methods are not implemented directly into the OpenQuake Engine or Model Building Toolkit, but simply in a standalone Python script.

2.1.3. Aftershock occurrence rates for a single mainshock

After the magnitude-frequency distribution for each mainshock has been defined, all the ruptures within some distance (e.g., four times the mainshock rupture length) of the mainshock are selected for consideration as aftershocks.

The conditional occurrence probabilities for each aftershock rupture, given the mainshock rupture, are calculated based on the aftershock magnitude-frequency distribution and the set of ruptures within the distance threshold. The criteria involved in this determination are the distances from the mainshock rupture to each aftershock rupture and the number of potential aftershock ruptures within each magnitude bin in the magnitude-frequency distribution.

For each aftershock rupture, an un-normalized conditional rupture probability $p'(rup_i|main)$ is defined based on the distance d_i from the mainshock rupture to the i^{th} aftershock rupture (accounting for the finite geometries of each), so that the probability decreases exponentially with distance:

$$p'(rup_i|main) = e^{d_i}$$

This probability is then normalized by the number of expected aftershocks in that magnitude bin $N(M_{aft})$ as derived from Eq. 2, and the sum of the un-normalized probabilities for all ruptures in the magnitude bin,

$$p(rup_i|main) = p'(rup_i|main) \cdot \frac{N(M_{aft})}{\sum p'(rup)} \qquad (3)$$

such that the sum of the normalized rupture probabilities is equal to $N(M_{aft})$.

Finally, the unconditional occurrence rate $r(rup_i)$ of some aftershock rupture i is calculated as the conditional occurrence probability times the occurrence rate of the mainshock:

$$r(rup_i) = p(rup_i|main) \cdot r(main)\,.$$

2.1.4. Aftershock occurrence rates for all mainshocks

The total aftershock occurrence rates for each rupture, considering all mainshocks, is simply the sum of the $r(rup_i)$ values for every mainshock in the model (or any mainshock above a threshold value for generating aftershocks). These rates are added to the occurrence rate of each mainshock before the classical PSHA computation is performed. This model is however not suitable for developing seismic aftershock PRA and not usable in the framework of the approach proposed here.

2.1.5. Generation of stochastic event sets with aftershocks

The methods developed here for classical PSHA with aftershocks need to be modified or extended to support the creation of stochastic event sets for single mainshock-aftershock sequences or for model-wide sequences. For this purpose, the calibration of the time-decay parameter of aftershock generation (which is not necessary for the time-independent classical method) is needed.

For any mainshock taken from the seismic source model, the code is in place to calculate the conditional earthquake occurrence probabilities for each potential aftershock ($p(rup_i|main)$ from Eq. 3).

If a specific mainshock rupture is selected, for example, for a single event-based seismic hazard and/or risk analysis, then the set of potential ruptures can be selected and the $p(rup_i|main)$ values for all ruptures can be calculated. Then, a temporal sequence can be constructed by modifying the $p(rup_i|main)$ values based on the time since the mainshock. Finally, stochastic sampling based on the final probabilities can be easily performed through standard methods.

If a model–wide stochastic event set including aftershocks is desired, then first a mainshock stochastic event set can be created from the seismic source model using existing tools in the OpenQuake Engine. Then, for each of those mainshocks, the aftershock sequences can be created as described in the

previous paragraph.

2.1.6. Conclusion

The methodology developed here, as implemented, adds an additional pre-analysis calculation to the Classical PSHA procedure. If the PSA or risk analysis depends on the results from a Classical PSHA, such as hazard curves or Uniform Hazard Spectra, then the PSA with aftershocks can proceed without any changes. However, this approach is not suitable for the seismic PRA for mainshock and aftershock sequences where an explicit sequence of earthquakes is needed for analysis (either a single mainshock-aftershock pair or a longer stochastic sequence of earthquakes). Then the proposed extension of the methods (described in Section 2.1.5) can be used.

2.2. Evaluation of Seismic Fragility

The seismic fragility of SSCs is evaluated using the assumption that seismic vibrations from the mainshock and aftershocks occur within a short period of time. Under this assumption, the modeled seismic impact as input ground motion is expressed by combining the seismic motion from the mainshock with one aftershock.

The combination of the mainshock and aftershocks with strong impact on NPP is selected from the combinations of the mainshock and aftershock models.

Seismic responses of NPP SSCs are calculated using the combination of mainshock + aftershock impacts, and fragility curves are estimated as a conditional failure frequency for a set level of input ground motions. The SSC response analysis models are the same as those used in the analysis considering only the mainshock.

To consider aftershock by conditional distributions (scenario-based analysis), conditional fragility curves need to be developed. An empirical correlation model can be used to generate aftershock spectra conditioned on different mainshock records.

In order to develop a methodology for the derivation of the damage-dependent fragility curves, which account for clustered seismicity and are suitable for use in the context of PSA, two approaches have been proposed: a damage state dependent approach by IUSS and a simplified shift-based approach by TUK.

For fragility calculations, the aftershock fragility needs to consider the damaged state from the mainshock, and the systems model should reflect the post-mainshock plant shutdown state.

2.2.1. Damage state dependent approach

In /D5.1/, a methodology was proposed that starts with hazard-consistent mainshock ground motion selection using Conditional Spectrum method. The proposed methodology consists of three steps. Firstly, for each mainshock ground motion, a compatible aftershock sequence is generated from the causative parameters of the mainshock event using the Epidemic-Type Aftershock Sequence (ETAS) model. Secondly, from the knowledge of the causative parameters of the selected aftershock, the response spectrum of the mainshock ground motion and the empirical variance-covariance matrix of the spectral accelerations of historical mainshock (MS) and aftershock (AS) ground motions recorded at the same station, the expected (target) MS-consistent AS response spectra are derived. This approach is not in agreement with the hazard assessment developed in 2.1.5. Real ground motions consistent with this target spectrum will then be extracted from the database (DB) of ground motions at our disposal. Thirdly, this exercise will be repeated for many MS events and a DB of pairs of MS ground motion records and MS-consistent AS ground motion records will be assembled. This DB of ground motion pairs will be used to create fragility curves that depend on the damage state of the structure after the MS event.

For implementing this methodology, definition of different damage states (DS) for every SSC is needed. So, a fragility curve will be developed for every DS of every SSCs based on the selected MS–AS sequence suite.

Figure 3 shows the damage dependent fragility functions obtained for a RC-ESDOF system through the above procedure. For the derivation of damage state-dependent fragility curves, up to four distinct DSs were considered with thresholds estimated from the yield and ultimate displacement capacity of the ESDOF system. The spectral displacement responses, obtained from subjecting the oscillators to each record of the selected the MS–AS sequences, were grouped together on the basis of the initial DS of the oscillator prior to the analysis. Fragility functions were then fit through maximum likelihood estimation for each initial DS, as described in /Papadopoulos et al. (2020)/.

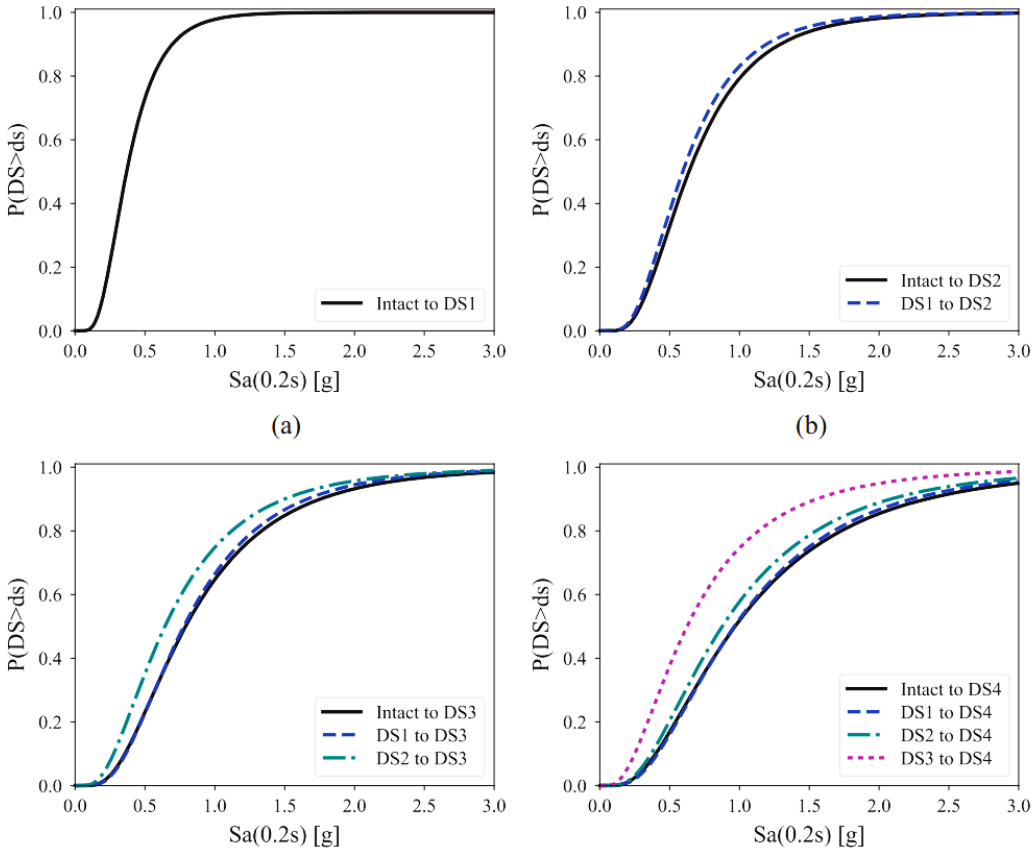

Figure 3: Damage-dependent fragility model for a RC-ESDOF system

2.2.2. Shift-based approach

The shift-based approach by TUK focuses on the changes in the fragility curve due to the additional damage of the mainshock. Since it is not dependent on the damage states and specific record selection of fragility calculation approaches, it offers a fast and simple prediction of the aftershock influence on the seismic fragility. The calculation of a simple shift in the curve, similar to a seismic margin, allows a simple integration in the current analysis approaches for NPPs. The procedure is illustrated in Figure 4 (see also /Mun C, Song J, 2022/).

The shift-based approach is based on the fact that the fragility curve of aftershock will shift to the left side of the fragility curve of mainshock because of structural damage due to the mainshock and lower intensity. The shift factor is calculated as a function of the mainshock damage to the intensity ratio:

Shift = F (Mainshock Damage/Intensity e.g., PGA)

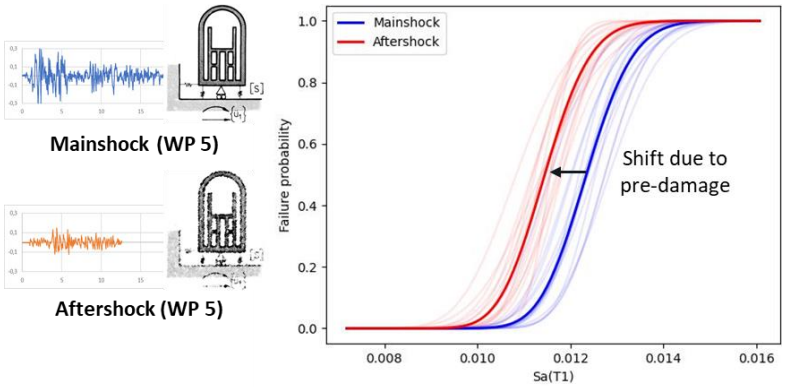

Figure 4: Shift-based approach for the quantification of aftershock impact on seismic fragilities

The shift-based approach based on classic method has double calculation time, but there is no need to define different damage states, which is the main problem in using the damage state approach for considering aftershock effects in SPSA of NPPs.

The final results of the approaches and the impact of considering aftershocks in seismic fragility analysis will be described in METIS Technical Report D6.6 "Influence of aftershocks and clustered seismicity on seismic fragility" within WP6.

2.3. System Analysis

After the component fragility curves have been plotted, the core damage frequency (CDF) can be calculated using the event and fault trees developed at the system reliability analysis stage. The procedure is the same as that used in SPSA for the mainshock.

Accepted international approaches to the performance of SPSA are provided in IAEA documents /IAEA SSG-3/, /IAEA-TECDOC-1937/. The general SPSA procedure is demonstrated in Figure 5.

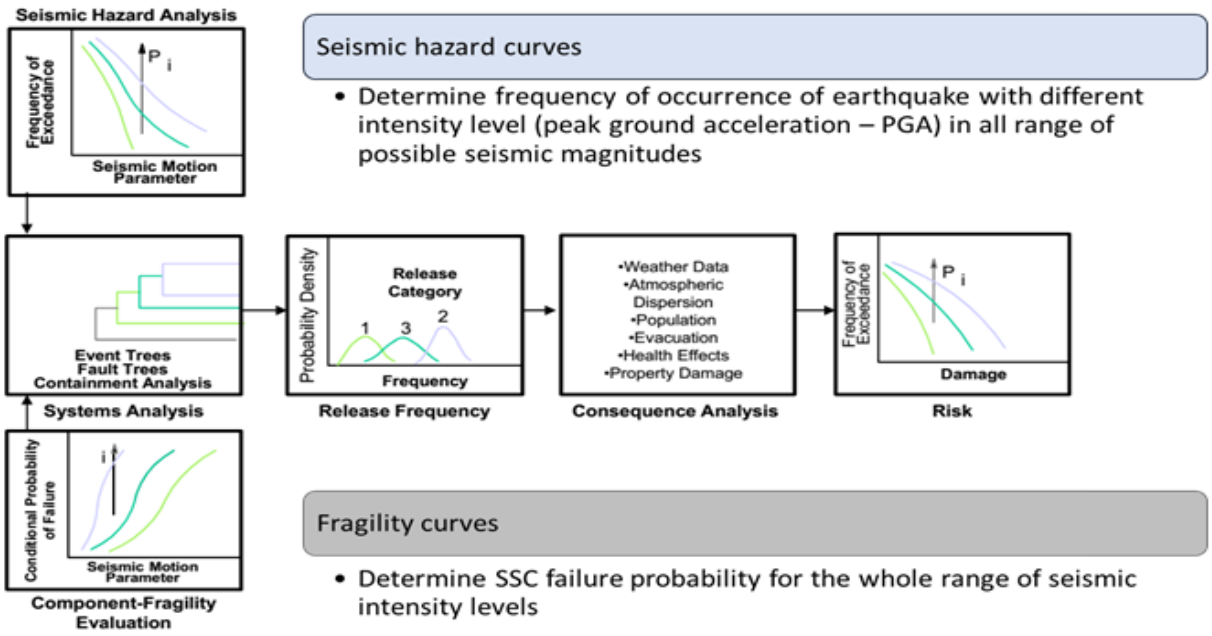

Figure 5: Stages of seismic PSA

Since SPSA considering aftershocks should also take into account the impact from the mainshock, the system analysis for aftershocks should take into account some aspects of modeling, which are discussed later in the section.

Emergency events to be taken into account in the event trees are those that have occurred in the period from the reactor emergency shutdown caused by the mainshock to the transition to cold shutdown state, as shown in Figure 6 (example of PWR). The estimated duration of the PWR transition to cold shutdown state is approximately 5 days (120 hours) /NEA/CSNI/.

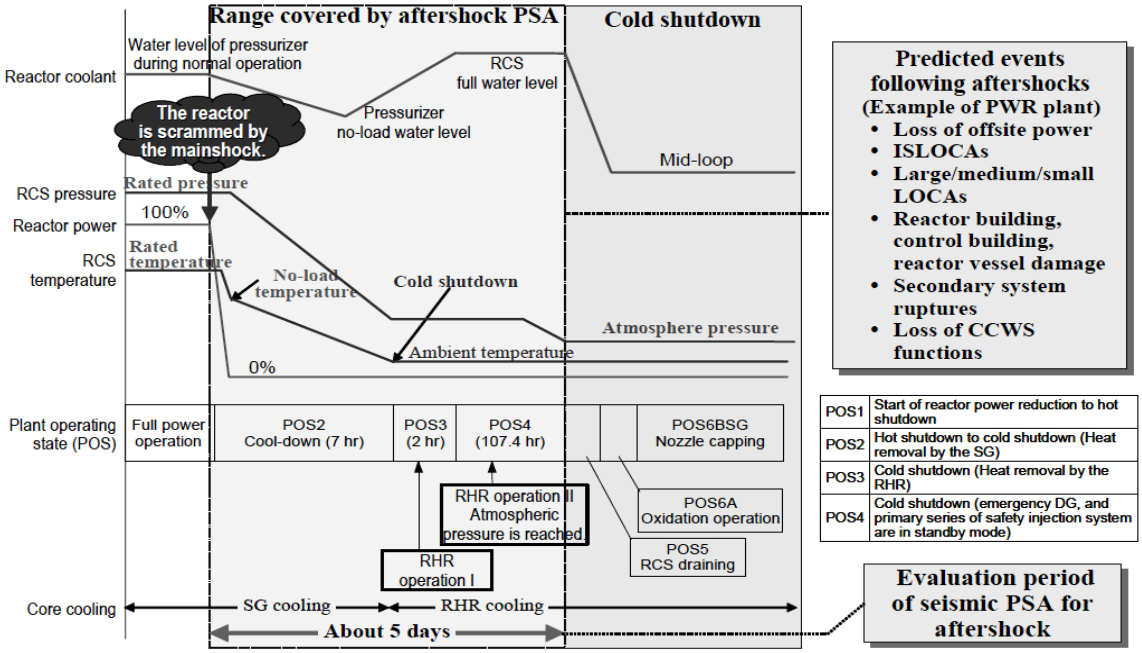

Figure 6: Predicted plant operating states following aftershocks (PWR plant)

At the same time, the average duration of WWER transition to cold shutdown for Zaporizhzhia NPP units is somewhat different from the proposed 5 days. The average duration of operational states for Zaporizhzhia NPP units is indicated in Table 2 /ZNPP/. As is seen, the total duration of OS1-OS7 that denote power decrease, reactor cooldown, and reduction to atmospheric pressure is approximately from 30 hours for unscheduled shutdown to 130 hours for scheduled shutdown.

No.	Operating state (OS)	OS duration for refueling outage	OS duration for unscheduled shutdown/events	OS duration for scheduled shutdown
1.	OS0 Full Power Operation			
2.	OS1 Reactor Power Decrease from 40% to Hot Zero Power and Reactor Transfer to Subcritical State	10.57	2.35	4.22
3.	OS2 Hot Shutdown or Semi-Hot Shutdown	1.82	10.73	42.35
4.	OS3 Reactor Cooldown to 200°C	5.60	0.76	1.42
5.	OS4 Reactor Cooldown from 200°C to 150°C	7.25	0.99	1.84
6.	OS5 Reactor Cooldown from 150°C to 140°C	1.81	0.25	0.46
7.	OS6 Reactor Cooldown from 140°C to 80°C	8.92	1.22	2.27
8.	OS7 Cold Shutdown without Primary System Depressurization	32.70	13.34	76.91
9.	OS8 Operation with Drained Primary System	575.17	0.00	0.00

Table 2: Duration of operating states (ZNPP)

Therefore, the time range for consideration of aftershocks in SPSA requires additional discussions in order to accept its optimal duration for correct account for the risks associated with aftershocks. The recommended period is plant transition to cold shutdown stable state, while time frame may vary depending on design and operational practices.

It should also be noted that in addition to impact on SSCs, aftershocks are important from the worker safety point of view. Specific concerns are: delayed initiation of needed activities (e.g., plant damage surveys) and interrupted ongoing work activities including recovery actions. Coordination challenges

have been experienced at NPPs (e.g., at Kashiwazaki-Kariwa (2007) and Onagava (2011)), and evacuation of some onsite personnel contributed to the lack of organizational knowledge (e.g., operation of equipment, location of items). This may have influence on modelling of human actions.

The scenarios are analyzed by the probabilistic method using a full-range PSA model for an NPP unit. For each level of seismic impacts, an event tree is developed to define the hierarchy of initiating events that may be caused by this particular impact, depending on their effect on the power unit (see Figure 7).

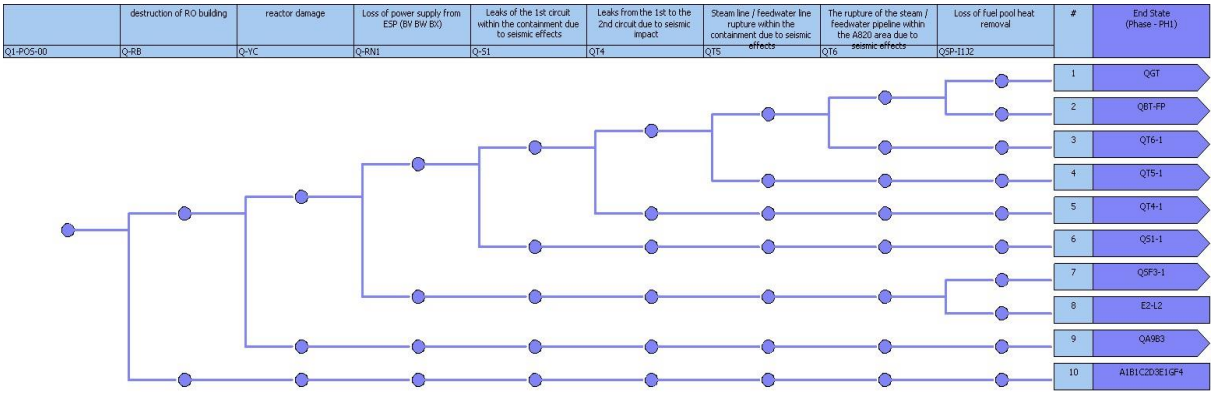

Figure 7: Example of an event tree for the mainshock

To assess aftershocks in accident sequences, success paths leading to cold shutdown are selected, excluding fault paths to be considered as core damage from the mainshock (see Figure 8). The event trees for aftershocks are modeled in the same way as for the mainshock, taking into account the power unit state.

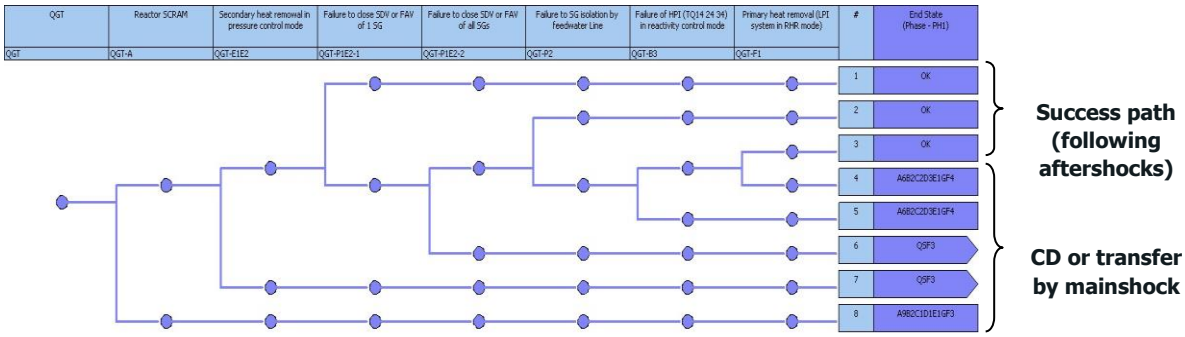

Figure 12: Analysis of accident sequences following aftershocks

Figure 8: Example of a general transient event tree

The fault trees should be modified in accordance with the /Committee/ recommendations: for each system component that is presented in the model, potential equipment failure caused by a random failure (defined in the equipment reliability database) and potential equipment failure caused by a seismic impact from the mainshock and aftershocks (see Figure 9) should be considered.

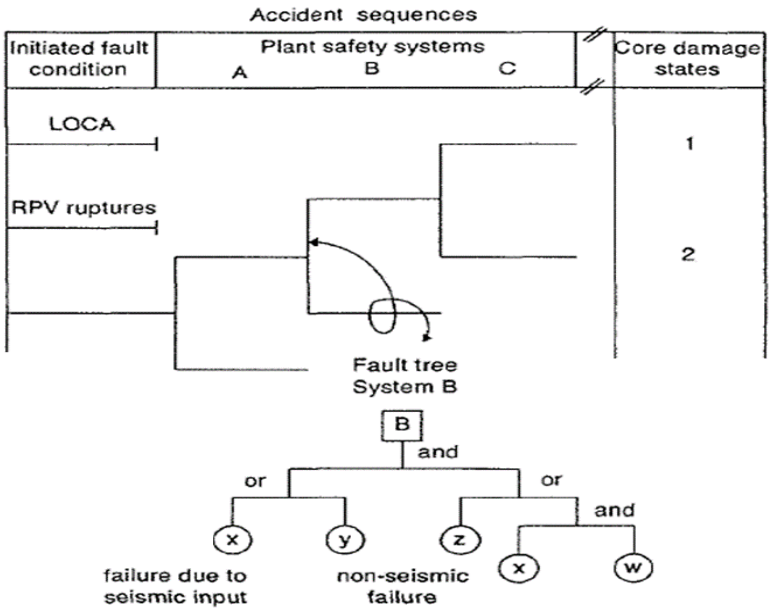

Figure 9: Schematic procedure to account for two types of equipment failure

To take into account the impact of aftershocks on SSCs, SSC failure caused by an aftershock is modeled in the fault trees. The probability of failure caused by an aftershock is estimated by multiplying the probability of zero failure (non-failure) of the SSC from the mainshock and the probability of its failure from the aftershocks: Pas=(1-Pms)*Pas, see Figure 10.

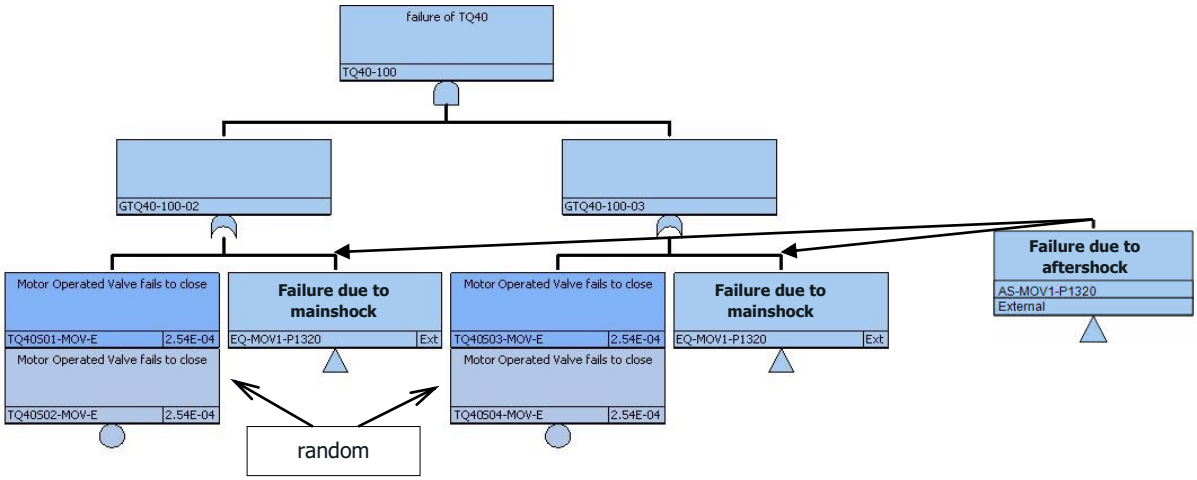

Figure 10: Example of considering aftershocks in the fault tree

The event trees and fault trees that consider the reliability of equipment for the mainshock and aftershocks are modified for all levels of seismic impacts that are taken into account in SPSA. Recovery actions of plant personnel and possible external assistance should also be taken into account.

The CDF caused by aftershocks is calculated using the fragility curve taking into account the impact of the mainshock and aftershocks and the aftershock hazard curve.

Results of the quantitative assessment for all levels of seismic impacts that are taken into account in SPSA are used to establish risk profiles from the mainshock and aftershocks. Corresponding study changes the timing of aftershocks and see whether there would be some time range when the effect of aftershocks will give significant risk increase. Such sensitivity studies may contribute to improving the severe accident management guides (SAMGs).

2.4. Important caveats that are recommended to be taken into account by developers of seismic PSA considering aftershocks

In considering the approaches to analyzing the influence of aftershocks on power units, the following caveats of METIS External Advisory Board /EAB/ members are very recommended to be taken into account.

The reason is that the most likely risks arising from seismic aftershocks would occur when the NPP is subjected to a mainshock larger than the design basis but smaller than one that would cause a core-damage accident. The concern is that some SSCs might suffer some damage – still not enough to cause them to fail to perform their safety function. Let's call this situation an "intermediate damage state" for those SSCs. Then, when the aftershock occurs later, the SSCs (now weaker than they should be) are more vulnerable, and the aftershock causes them to fail.

For a "full aftershock seismic PSA" to provide the usual insights expected from a seismic PSA (core-damage frequency sequence-by-sequence, principal contributors, etc.), it would be required to analyze accident sequences where one or more SSCs are in an "intermediate damage state" arising from the mainshock. The initial condition for the aftershock SPSA is that the SSC still performs its safety function but is weakened. However, developing a full-scope aftershock seismic PSA may be too complex and resource-consuming and is unlikely to provide useful safety insights.

At the beginning of the analysis, we have essentially zero information on how to characterize those "intermediate damage state" situations. Their characterization would depend on how large the mainshock is, what the "intermediate damage state" looks like, and how much additional seismic ground motion is required to cause failure. The way to gain that information, for equipment, would be an extremely elaborate shake-table complex testing program (the number of components to be included in such a PSA is probably large).

Many issues would require shake-table testing. One would need shake-table testing that causes some damage but it is lower at input levels than the "damage threshold" defined as "the SSC cannot perform the safety function." That would be the intermediate state of the item after the mainshock but before the aftershock. Then the shake-table experimenter would need to take that equipment item, partially damaged by the simulated main earthquake, and shake it more (the aftershock) until it truly cannot perform its safety function. In the absence of such information, assumptions made regarding the damage states will drive the results. But without that data, a realistic full aftershock seismic PSA is not feasible.

The other way is to perform a "conservative" or "simplified" SPSA using demonstrably conservative PSA-type analyses or simplified PSA evaluations, but keeping a target objective of achieving realistic safety significance (or not) of aftershocks consistently with experience feedback and observations. For example, after analyzing the plant design, safe shutdown paths, etc., SSCs that can be potentially damaged in the event of a mainshock of specific level are selected (i.e., the corresponding damage is "assigned" to them). Further, failures in the event of an aftershock are "assigned" to the selected SSCs, which will accordingly influence the change in their fragility curves in relation to those used in the mainshock SPSA. Aftershock SPSA is then performed according to the procedure described in this Strategy. It should be taken into account that the assignment of damage/failure to SSCs strongly depends on the site seismic intensity level (levels of considered mainshocks and aftershocks).

It should also be noted that the proposed methods discussed in Sections 2.1-2.3 of this Strategy are still in formative stages and have not been fully evaluated or applied. The six challenges (added in the Introduction) that are involved in a rigorous aftershock analysis should be considered to get some practical insights and make judgments whether a rigorous aftershock analysis needs to be conducted at all.

There is one more very important type of information that can be obtained using SPSA tools: the safety concern is that a mainshock has not caused a core-damage accident, but an aftershock would

do so, because some SSCs are weakened. The information that could be derived using SPSA tools, given the appropriate guidance, is identification of those SSCs that are both required in terms of their post-mainshock seismic safety function and also might find themselves in a seriously weakened "intermediate damage state." These would be the SSCs to worry about vis-a-vis aftershocks. Once those are identified, it should be feasible to direct the plant staff, in the immediate aftermath (first few hours) after the mainshock, to inspect each such SSC and determine whether (or not) it has been seriously damaged (even though it still performs its safety function) and, if so, whether anything can and should be done for that SSC to help keep the plant safe if an aftershock were to occur. The list of SSCs to inspect urgently should be short, and very high priority could be assigned to examining them.

The example presented in the Appendix to this Strategy includes proposals to sensitivity analysis that can be conducted to identify potential vulnerable SSCs and situations. Critical SSCs which make the highest contribution to CDF according to the test calculations using software tools were considered. This is a challenge for SPSA developers considering aftershocks to choose and substantiate such SSCs and their "intermediate damage state". Some items which are important for analysts are as follows:

- Selection of mainshock and aftershock characteristics for the sensitivity analysis (for example, from a deaggregation of hazard, selection of a reference earthquake etc.).
- Selection of critical safety functions, in case that the plant has been successfully shut down (for situations where no core damage has occurred) after an mainshock and continued cooldown is important.
- Selection of critical systems and subsystems to fulfill the required safety functions (for example, RHR and supporting systems). In this regard, availability of a shutdown PRA can provide very useful guidance.
- Identification and evaluation of the post-mainshock status of SSCs associated with the above systems that are vulnerable to damage.
- Estimate of the fragility shift (where applicable).
- Practical insights and recommendations/indications which can be determined as a result of SPSA considering aftershocks.

3. Conclusions

The Strategy describes approaches used to analyze the seismic hazard of aftershocks, evaluate the fragility of NPP SSCs from the mainshock and aftershocks, and analyze the system reliability taking into account additional impacts associated with aftershocks after the emergency shutdown caused by the mainshock.

There is limited report on the impact of aftershocks on power plants and their SSCs (although references and bibliography especially focus on assessing damage due to earthquake events). However, existing reports show that aftershocks in general do not directly cause additional damage to SSCs that have been properly designed to withstand seismic loads. This indicates that aftershocks should not be considered a significant safety issue for these sets of SSCs, based on available experience feedback. Instead, aftershocks might cause further damage to subsystems that were already weakened by the mainshock, essentially those without a proper seismic design (e.g. masonry structures or subsystems that were not properly aligned as a result of the mainshock). This may lead to focus post-mainshock inspections to these kinds of SSCs, in particular those that may have interaction issues with safety related SSCs.

Based on the review of literature sources and various databases highlighting past seismic events and the resulting experience feedback and lessons learned, the Strategy proposes a conservative simplified SPSA approach for consideration of aftershocks in seismic PSA.

To assess the seismic hazard of aftershocks, a model should be developed for stochastic prediction of aftershock activity. The first step in the process of calculating the aftershock occurrence rates is to estimate the aftershock productivity parameters. This step should come after the seismic catalogue has been declustered and requires the association of aftershocks removed in the declustering process with the causative mainshock. This association is not always part of the declustering procedure, depending on the methods used, so additional post-declustering analysis of the mainshock and aftershock catalogues may be necessary. After the magnitude-frequency distribution for each mainshock has been defined, all the ruptures within some distance of the mainshock are selected for consideration as aftershocks (for more details, see para 2.1).

The seismic fragility of SSCs is evaluated using the assumption that seismic excitations from the mainshock and aftershocks occur within a short period of time. Under this assumption, the modeled seismic impact as input ground motion is expressed by combining the seismic motion from the mainshock with one aftershock. Seismic responses of NPP SSCs are calculated using the combination of mainshock + aftershock impacts, and fragility curves are estimated as a conditional failure frequency for a set level of input ground motions. The SSC response analysis models are the same as those used in the analysis considering only the mainshock. To consider aftershock by conditional distributions (scenario-based analysis), conditional fragility curves need to be developed. Two approaches have been proposed in this Strategy: a damage state dependent approach and a simplified shift-based approach. For implementing the first one, the definition of different damage states for every SSC is needed. So, a fragility curve will be developed for every DS of every SSC based on the selected MS–AS sequence suite. The shift-based approach focuses on changes in the fragility curve due to the additional damage of the mainshock. The fragility curve of the aftershock will shift to the left side of the fragility curve of the mainshock because of the structural damage due to the mainshock and lower intensity (for more details, see para 2.2). The final results of the approaches and the impact of considering aftershocks in seismic fragility analysis will be described in METIS Technical Report D6.6 "Influence of aftershocks and clustered seismicity on seismic fragility" within WP6.

After the component fragility curves have been plotted, the core damage frequency (CDF) can be calculated using the event and fault trees developed at the system reliability analysis stage. Emergency events to be taken into account in the event trees are those that have occurred in the period from the reactor emergency shutdown caused by the mainshock to the transition to cold shutdown state. The time range for consideration of aftershocks in SPSA requires additional discussions in order to accept its optimal duration for correct account for the risks associated with aftershocks. The scenarios are analyzed by the probabilistic method using a full-range PSA model for

an NPP unit. To assess aftershocks in accident sequences, success paths leading to cold shutdown are selected, excluding fault paths to be considered core damage from the mainshock. The event trees for aftershocks are modeled in the same way as for the mainshock, taking into account the power unit state. To take into account the impact of aftershocks on SSCs, SSC failure caused by an aftershock is modeled in the fault trees. The probability of failure caused by an aftershock is estimated by multiplying the probability of zero failure (non-failure) of the SSC from the mainshock and the probability of its failure from the aftershocks. Recovery actions of plant personnel and possible external assistance should also be taken into account. The CDF caused by aftershocks is calculated using the fragility curve taking into account the impact of the mainshock and aftershocks and the aftershock hazard curve.

The final goal of this activity is to provide the international community with safety insights regarding aftershocks, consistent with post-earthquake experience feedback, such as i) practical approaches to identifying SSCs that could be sensitive to aftershocks, ii) screening out less important issues, and iii) possibly providing post-mainshock inspection procedures.

The test calculation results showed that the aftershock made a small contribution to the core damage frequency for the low intensity area of Zaporizhzhia NPP Unit 1 SPSA (test case performed to support the Strategy): lower than 1% in the SAPHIRE test model and about 2% in the RiskSpectrum PSA test model (see the Appendix). For test calculation to determine the influence of aftershock on CDF considering the "intermediate damage state" of the ZNPP Unit 1 reactor compartment building, combinations of seismic effects were addressed. The contribution to the core damage frequency was assessed for the following combination: mainshock with PGA=0.5g and 3.61E-06 frequency and subsequent aftershock with PGA=0.3g and 5.00E-01 postulated probability after the mainshock reached ~ 11% (see the Appendix)[1].

Before starting the SPSA analysis considering aftershocks, the caveats indicated in Chapter 2 (para 2.4) are very recommended to be taken into account.

Based on the analyses performed during the development of this Strategy, the following key notes could be recommended for future studies of considering aftershocks in SPSA:

1) The goal of an aftershock evaluation would be to identify SSCs necessary to maintain the plant in a safe shutdown state and assess their potential vulnerability to aftershocks or perhaps to guide post-earthquake inspections.

2) Significant challenges exist in developing fragilities for SSCs that consider the damage state due to the mainshock. For SSCs not damaged by the mainshock, the fragility should be the same as before the mainshock.

3) The systems model should simulate the post-earthquake shutdown state of the plant.

Future research into these areas would be necessary to optimize aftershock SPSA evaluations and determine the appropriate insights.

[1] It should be noted that these conclusions are valid just for the test case considered.

4. Acknowledgments

We want to thank Robert Budnitz, Nilesh Chokshi, and John Richards (members of the METIS External Advisory Board) for very valuable comments and recommendations which were accounted in this Strategy and also Irmela Zentner, Emmanuel Viallet for the great organizational work to discuss aftershock impact and its possible consideration in seismic PSA during the Strategy development.

5. Bibliography

/Chi Chi Taiwan/ Investigation of the 1999 Chi Chi Taiwan Earthquake, EPRI, Palo Alto, CA: 2001.

/Raceway Systems/ The Performance of Raceway Systems in Strong-Motion Earthquakes, EPRI, Palo Alto, CA: 1991.

/Manzanillo/ Earthquake of October 9, 1995: Effects at the Manzanillo Power Plant, EPRI, Palo Alto, CA: 1997.

/Northridge Earthquake/ The January 17, 1994, Northridge Earthquake: Effects on Electric Power and Selected Industrial Facilities, EPRI, Palo Alto, CA: 1997.

/Turkey Earthquake/ Investigation of the 1999 Kocaeli Turkey Earthquake: Effects on Power and Industrial Facilities, EPRI, Palo Alto, CA: 2001. 1003119.

/SMART 2013/ Benjamin Richard, Stefano Cherubini, François Voldoire, Pierre-Etienne Charbonnel, Thierry Chaudat, et al. SMART 2013: Experimental and numerical assessment of the dynamic behavior by shaking table tests of an asymmetrical reinforced concrete structure subjected to high intensity ground motions. Engineering Structures, 2016, 109, pp. 99-116.

/Earthquake at Kashiwazaki-Kariwa NPP/ Preliminary Findings and Lessons Learned from the 16 July 2007 Earthquake at Kashiwazaki-Kariwa NPP, IAEA, AT: 2007.

/Niigata-Chuetsu Oki, Japan/ Kayen, R., Collins, B.D., Abrahamson, N., Ashford, S., Brandenberg, S.J., Cluff, L., Dickenson, S., Johnson, L., Kabeyasawa, T., Kawamata, Y., Koumoto, H., Marubashi, N., Pujol, S., Steele, C., Sun, J., Tanaka, Y., Tokimatsu, K., Tsai, B., Yanev, P., Yashinsky, M., and Yousok, K., 2007. Investigation of the M6.6 Niigata-Chuetsu Oki, Japan, Earthquake of July 16, 2007: U.S. Geological Survey, Open File Report 2007-1365, 230 pg.

/Kashiwazaki-Kariwa NPP, IAEA. 2007/ Preliminary Findings and Lessons Learned from the 16 July 2007 Earthquake at Kashiwazaki-Kariwa NPP (Volume I, II), IAEA, AT: 2007.

/Tohoku earthquake and tsunami, Japan/ IAEA mission to Onagawa nuclear power station to examine the performance of systems, structures and components following the great east Japanese earthquake and tsunami, IAEA, AT: 2012.

/Mun C, Song J, 2022/ Mun C, Song J. Probabilistic Modelling of Condensate Storage Tanks under Sequence of Main and Aftershocks Using Bayesian Network, SMiRT-26, Berlin/Potsdam, Germany, July 10-15, 2022. https://repository.lib.ncsu.edu/server/api/core/bitstreams/9ca9cd26-275c-41d3-8487-e86de4f7c03b/content

/JNES/ Development of Seismic PSA Methodology Considering Aftershock, Hideaki TSUTSUMI, Hideo NANBA, Shohei MOTOHASHI, Katsumi EBISAWA, Japan Nuclear Energy Safety Organization (JNES)

/EAB/ Aftershock analysis. Robert Budnitz, Nilesh Chokshi, and John Richards (members of the METIS External Advisory Board), e-mail to Irmela Zentner, copy to Emmanuel Viallet, 19 January, 2023.

/Felzer, Abercrombie, and Ekstrom 2004/ Felzer, Karen R, Rachel E Abercrombie, and Goran Ekstrom. 2004. "A Common Origin for Aftershocks, Foreshocks, and Multiplets." Bulletin of the Seismological Society of America 94 (1): 88–98.

/ NEA/CSNI/ Specialist Meeting on The Seismic Probabilistic Safety Assessment of Nuclear Facilities, SEOGWIPO ICC, Jeju Island, Korea, 6-8 November 2006, NEA/CSNI/R(2007)14 (2007).

/D5.1/ Methodology for site specific rockhazard consistent record. METIS - D5.1 - Issued on 2022-09-21

/Papadopoulos et al. (2020)/ Kohrangi, M., Papadopoulos, A. N., Bazzurro, P., & Vamvatsikos, D. (2020). Correlation of spectral acceleration values of vertical and horizontal ground motion pairs. Earthquake Spectra. https://doi.org/10.1177/8755293020919416

/IAEA SSG-3/ Development and Application of Level 1 Probabilistic Safety Assessments for Nuclear Power Plants. IAEA Specific Safety Guide No. SSG-3. Vienna: IAEA, 2010. 195 p.

/IAEA-TECDOC-1937/ Probabilistic Safety Assessment for Seismic Events. IAEA-TECDOC-1937. Vienna: IAEA, 2020. 106 p.

/ZNPP/ Zaporizhzhia NPP. Power Unit 6. Safety Analysis Report. Living Probabilistic Safety Assessment for a Full Range of Events for ZNPP Unit 6, 21.6.59.OB.04-19.

/Committee/ The Headquarters for Earthquake Research Promotion, Earthquake Research Committee: AFTERSHOCK PROBABILITY EVALUATION METHODS, APRIL 8, 1998.

/EPRI 1019200/ EPRI Report 1019200 (2009). Seismic fragility applications guide update. Electric Power Research Institute Final Report. Palo Alto, CA.

Appendix. Example application of PSA considering aftershocks to assess their impact on risk

1 Preliminary test modeling of aftershocks

The test modeling of aftershocks was performed using the SAPHIRE and RiskSpectrum PSA software tools for Zaporizhzhia NPP Unit 1, taking into account the following input data and assumptions:

- unit state POS0 "Operation at full power" during the mainshock;
- group of initiating events QS1 "Primary leaks in containment S1, S2, S3";
- mainshock Q4 with PGA=0.3g and 2.00E-05 frequency;
- aftershock AS (A1) with PGA=0.17g and 5.00E-01 postulated probability after the mainshock;
- accident sequences that lead to damage of the reactor core resulting from the mainshock are not considered in the aftershock analysis.

For the test modeling, the model and input data (including the SSC fragility curves) of the Zaporizhzhia NPP Unit 1 SPSA were used.

The SAPHIRE model does not take into account operation of the hydroaccumulator system (YT) in the event tree for the aftershock because it is assumed that the hydroaccumulators would operate for a short period of time after the mainshock in case of large leaks (S1). Conversely, the RiskSpectrum model takes into account the operation of hydroaccumulators in the event tree for the aftershock.

These modeling options for the initiating event "Primary leaks" can be considered to be simulation of two different independent aftershocks in terms of their time of occurrence after the mainshock. One option is when the aftershock occurs immediately after the mainshock (within several hours). The second option is when the aftershock occurs within a longer time after the mainshock.

The calculation results showed that the aftershock of accepted intensity made a small contribution to the core damage frequency for SPSA: lower than 1% in the SAPHIRE test model and about 2% in the RiskSpectrum PSA test model (see below).

1.1 Example of aftershock modeling in SAPHIRE software

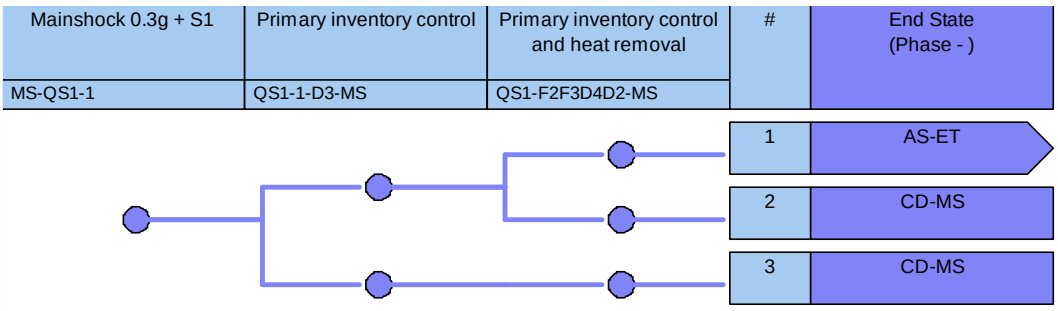

Figure A.1: Event tree MS-QS1-1 (0.3g) for S1, S2, S3 LOCAs considering aftershock AS (0.17g)

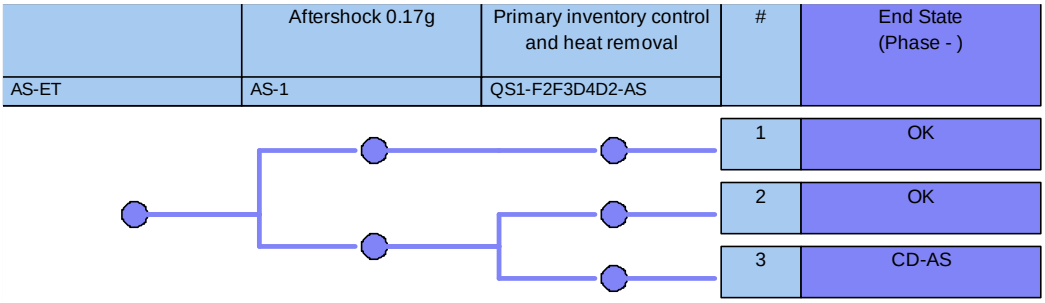

Figure A.2: Event tree AS-ET for aftershock AS (0.17g)

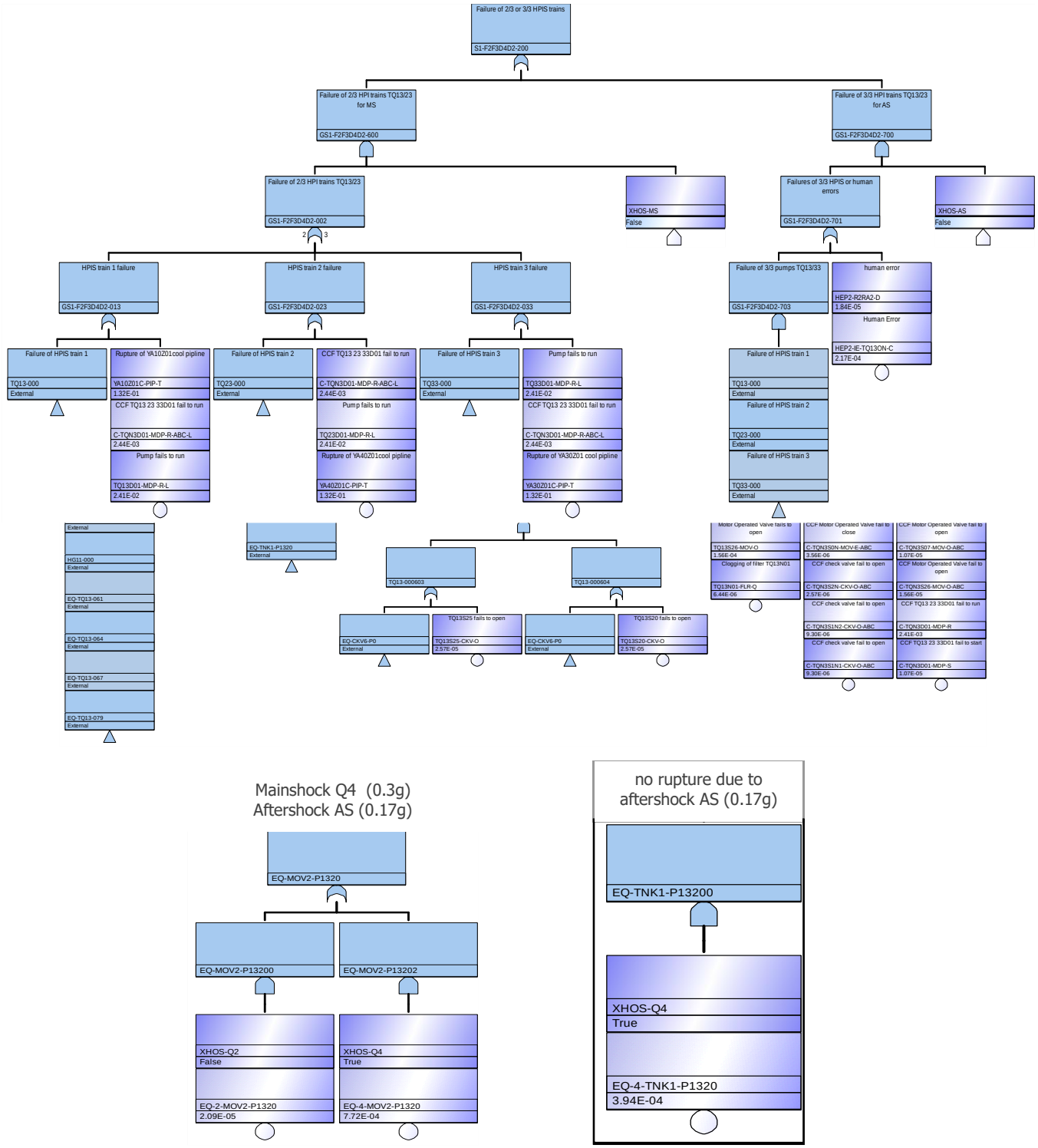

Figure A.3: Consideration of failures (ruptures) of components / piping in aftershock AS

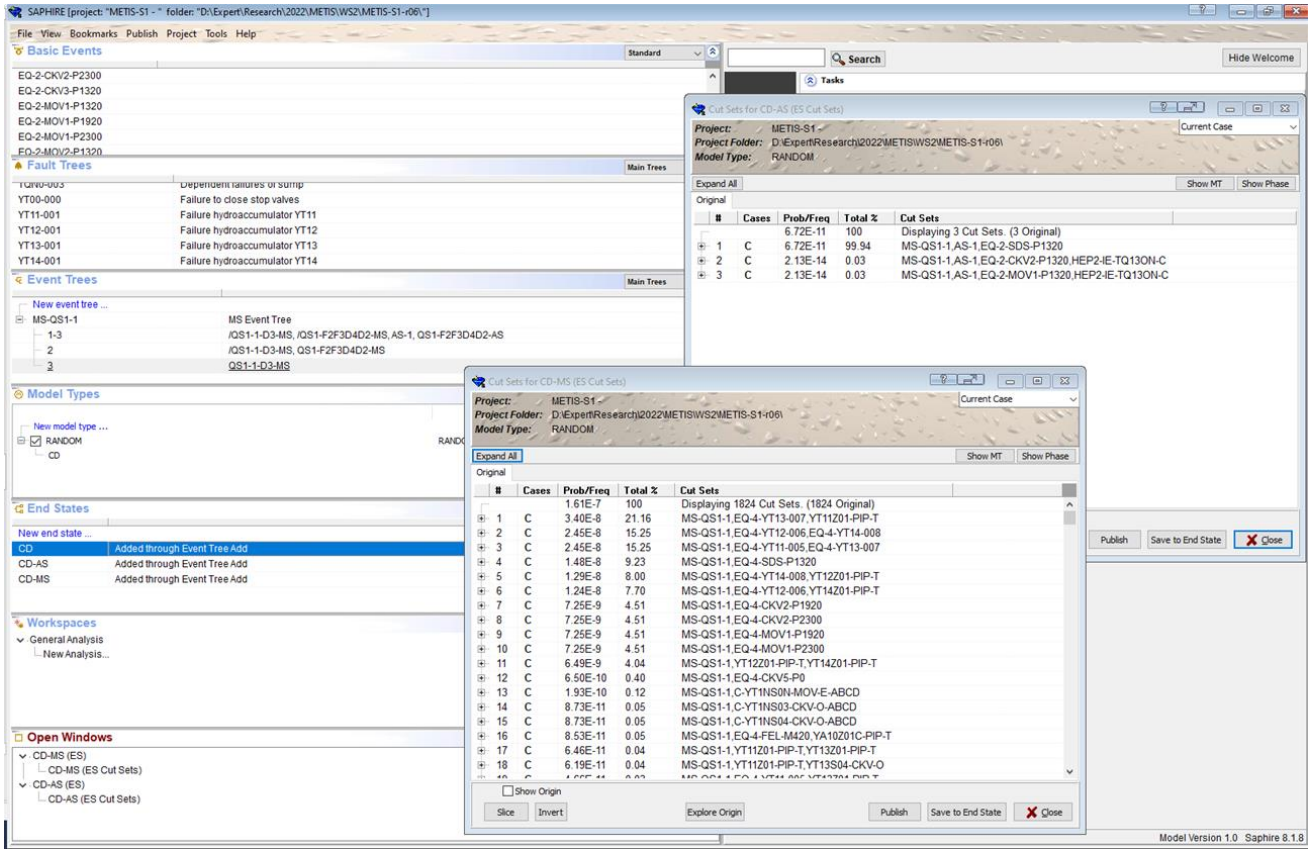

Figure A.4: Results of analysis using the SAPHIRE testing model

1.2 Example of aftershock modeling in RiskSpectrum PSA software

S1, S2, S3 LOCAs from primary circuit to the containment	Primary inventory control (YT)	Primary inventory control and heat removal (LPIS or HPI)	Aftershock A1 (0.17g)				
QS	QS-D3	QS-F2F3D4D2	QS-A1	No.	Freq.	Conseq.	Code
				1		OK	
				2		QS-A1	QS-A1
				3		CDF-MS	QS-F2F3D4D2
				4		CDF-MS	QS-D3

Figure A.5: Event tree QS (0.3g) for S1, S2, S3 LOCAs considering aftershock A1 (0.17g)

Aftershock A1 (0.17g)	Primary inventory control (YT)	Primary inventory control and heat removal (LPIS or HPI)				
QS-A1	QS-A1-D3	QS-A1-F2F3D4D2	No.	Freq.	Conseq.	Code
			1		OK	
			2		CDF-AS	QS-A1-F2F3D4D2
			3		CDF-AS	QS-A1-D3

Figure A.6: Event tree QS-A1 for aftershock A1 (0.17g)

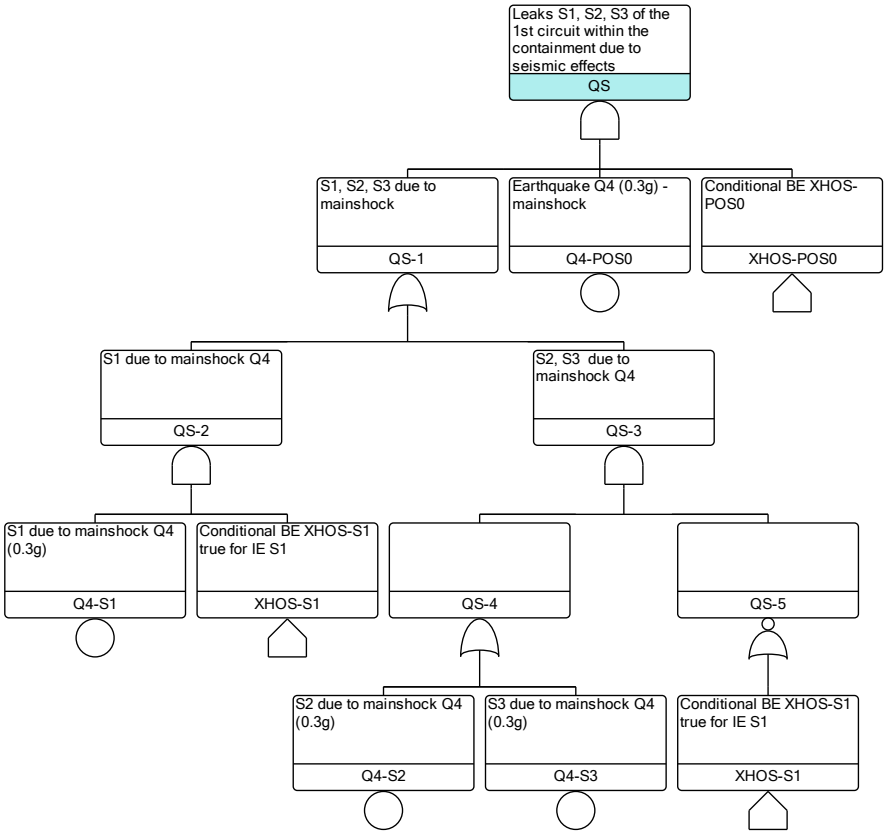
Leaks S1, S2, S3 of the 1st circuit within the containment due to seismic effects
QS
S1, S2, S3 due to mainshock
QS-1
Earthquake Q4 (0.3g) - mainshock
Q4-POS0
Conditional BE XHOS-POS0
XHOS-POS0
S1 due to mainshock Q4
QS-2
S2, S3 due to mainshock Q4
QS-3
S1 due to mainshock Q4 (0.3g)
Q4-S1
Conditional BE XHOS-S1 true for IE S1
XHOS-S1
QS-4
QS-5
S2 due to mainshock Q4 (0.3g)
Q4-S2
S3 due to mainshock Q4 (0.3g)
Q4-S3
Conditional BE XHOS-S1 true for IE S1
XHOS-S1

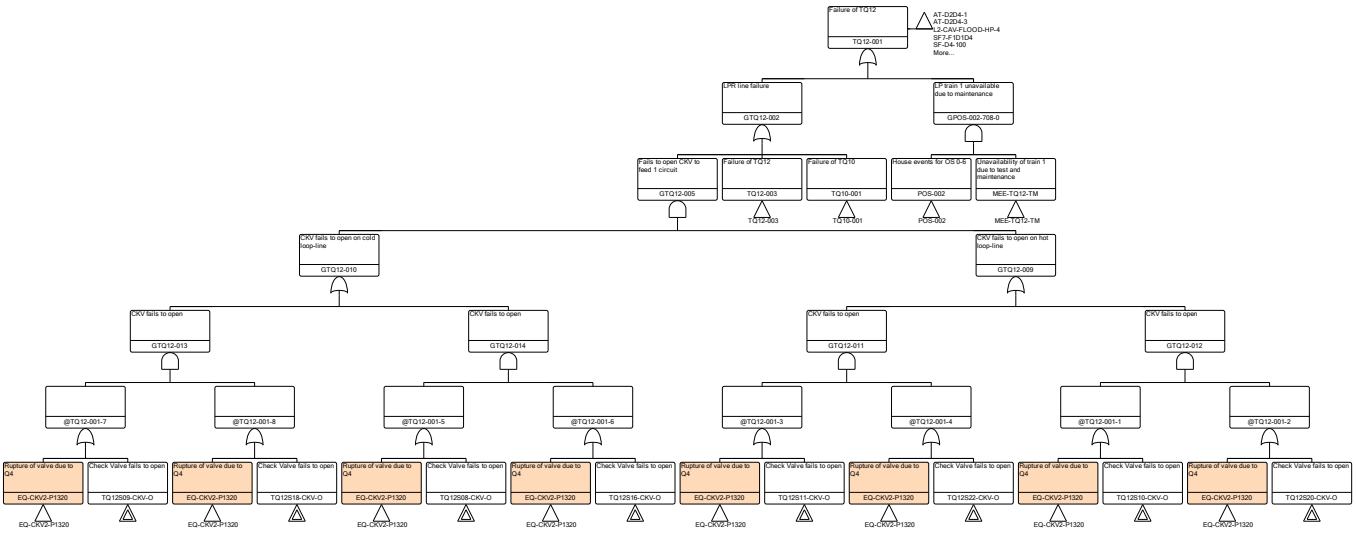

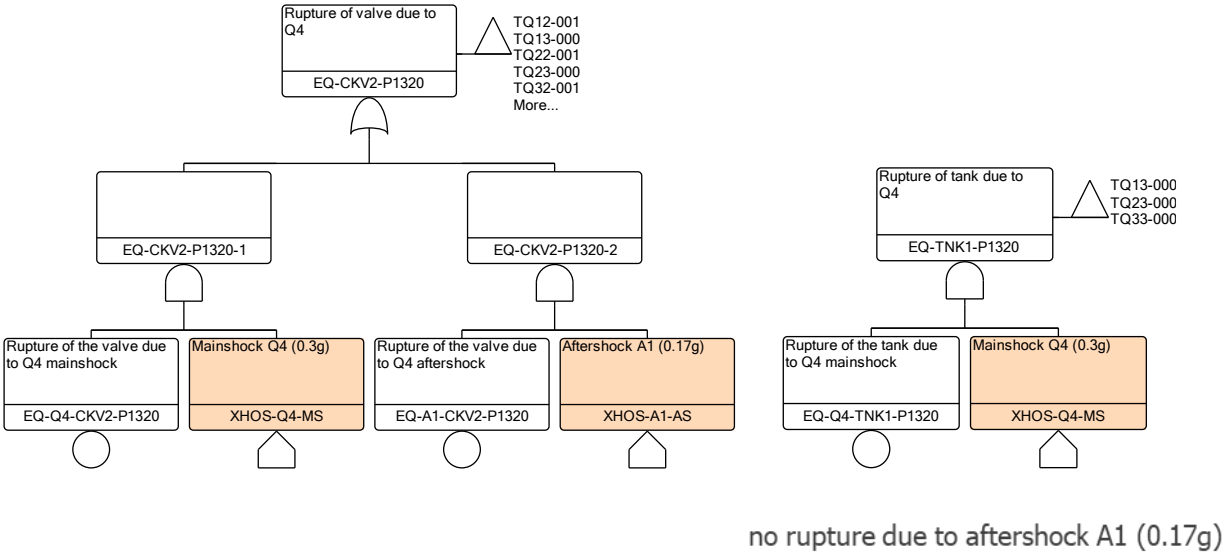

Figure A.7: Consideration of failures (ruptures) of components / piping in accident sequences of aftershock A1

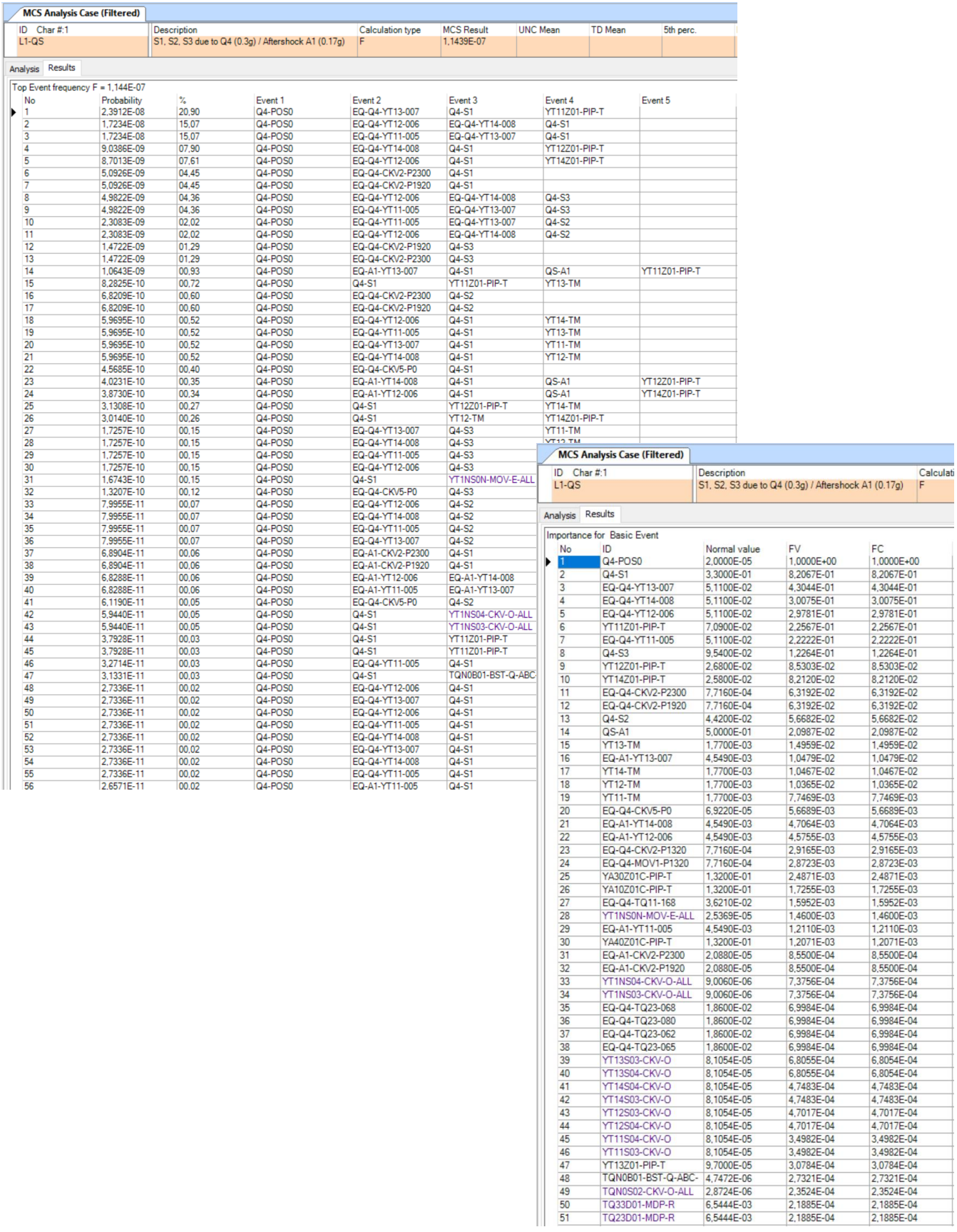

MCS Analysis Case (Filtered)

ID Char #:1	Description	Calculation type	MCS Result	UNC Mean	TD Mean	5th perc.
L1-QS	S1, S2, S3 due to Q4 (0.3g) / Aftershock A1 (0.17g)	F	1,1439E-07			

Analysis | Results

Top Event frequency F = 1,144E-07

No	Probability	%	Event 1	Event 2	Event 3	Event 4	Event 5
1	2,3912E-08	20,90	Q4-POS0	EQ-Q4-YT13-007	Q4-S1	YT11Z01-PIP-T	
2	1,7234E-08	15,07	Q4-POS0	EQ-Q4-YT12-006	EQ-Q4-YT14-008	Q4-S1	
3	1,7234E-08	15,07	Q4-POS0	EQ-Q4-YT11-005	EQ-Q4-YT13-007	Q4-S1	
4	9,0386E-09	07,90	Q4-POS0	EQ-Q4-YT14-008	Q4-S1	YT12Z01-PIP-T	
5	8,7013E-09	07,61	Q4-POS0	EQ-Q4-YT12-006	Q4-S1	YT14Z01-PIP-T	
6	5,0926E-09	04,45	Q4-POS0	EQ-Q4-CKV2-P2300	Q4-S1		
7	5,0926E-09	04,45	Q4-POS0	EQ-Q4-CKV2-P1920	Q4-S1		
8	4,9822E-09	04,36	Q4-POS0	EQ-Q4-YT12-006	EQ-Q4-YT14-008	Q4-S3	
9	4,9822E-09	04,36	Q4-POS0	EQ-Q4-YT11-005	EQ-Q4-YT13-007	Q4-S3	
10	2,3083E-09	02,02	Q4-POS0	EQ-Q4-YT11-005	EQ-Q4-YT13-007	Q4-S2	
11	2,3083E-09	02,02	Q4-POS0	EQ-Q4-YT12-006	EQ-Q4-YT14-008	Q4-S2	
12	1,4722E-09	01,29	Q4-POS0	EQ-Q4-CKV2-P1920	Q4-S3		
13	1,4722E-09	01,29	Q4-POS0	EQ-Q4-CKV2-P2300	Q4-S3		
14	1,0643E-09	00,93	Q4-POS0	EQ-A1-YT13-007	Q4-S1	QS-A1	YT11Z01-PIP-T
15	8,2825E-10	00,72	Q4-POS0	Q4-S1	YT11Z01-PIP-T	YT13-TM	
16	6,8209E-10	00,60	Q4-POS0	EQ-Q4-CKV2-P2300	Q4-S2		
17	6,8209E-10	00,60	Q4-POS0	EQ-Q4-CKV2-P1920	Q4-S2		
18	5,9695E-10	00,52	Q4-POS0	EQ-Q4-YT12-006	Q4-S1	YT14-TM	
19	5,9695E-10	00,52	Q4-POS0	EQ-Q4-YT11-005	Q4-S1	YT13-TM	
20	5,9695E-10	00,52	Q4-POS0	EQ-Q4-YT13-007	Q4-S1	YT11-TM	
21	5,9695E-10	00,52	Q4-POS0	EQ-Q4-YT14-008	Q4-S1	YT12-TM	
22	4,5685E-10	00,40	Q4-POS0	EQ-Q4-CKV5-P0	Q4-S1		
23	4,0231E-10	00,35	Q4-POS0	EQ-A1-YT14-008	Q4-S1	QS-A1	YT12Z01-PIP-T
24	3,8730E-10	00,34	Q4-POS0	EQ-A1-YT12-006	Q4-S1	QS-A1	YT14Z01-PIP-T
25	3,1308E-10	00,27	Q4-POS0	Q4-S1	YT12Z01-PIP-T	YT14-TM	
26	3,0140E-10	00,26	Q4-POS0	Q4-S1	YT12-TM	YT14Z01-PIP-T	
27	1,7257E-10	00,15	Q4-POS0	EQ-Q4-YT13-007	Q4-S3	YT11-TM	
28	1,7257E-10	00,15	Q4-POS0	EQ-Q4-YT14-008	Q4-S3	YT12-TM	
29	1,7257E-10	00,15	Q4-POS0	EQ-Q4-YT11-005	Q4-S3		
30	1,7257E-10	00,15	Q4-POS0	EQ-Q4-YT12-006	Q4-S3		
31	1,6743E-10	00,15	Q4-POS0	Q4-S1	YT1NS0N-MOV-E-ALL		
32	1,3207E-10	00,12	Q4-POS0	EQ-Q4-CKV5-P0	Q4-S3		
33	7,9955E-11	00,07	Q4-POS0	EQ-Q4-YT12-006	Q4-S2		
34	7,9955E-11	00,07	Q4-POS0	EQ-Q4-YT14-008	Q4-S2		
35	7,9955E-11	00,07	Q4-POS0	EQ-Q4-YT11-005	Q4-S2		
36	7,9955E-11	00,07	Q4-POS0	EQ-Q4-YT13-007	Q4-S2		
37	6,8904E-11	00,06	Q4-POS0	EQ-A1-CKV2-P2300	Q4-S1		
38	6,8904E-11	00,06	Q4-POS0	EQ-A1-CKV2-P1920	Q4-S1		
39	6,8288E-11	00,06	Q4-POS0	EQ-A1-YT12-006	EQ-A1-YT14-008		
40	6,8288E-11	00,06	Q4-POS0	EQ-A1-YT11-005	EQ-A1-YT13-007		
41	6,1190E-11	00,05	Q4-POS0	EQ-Q4-CKV5-P0	Q4-S2		
42	5,9440E-11	00,05	Q4-POS0	Q4-S1	YT1NS04-CKV-O-ALL		
43	5,9440E-11	00,05	Q4-POS0	Q4-S1	YT1NS03-CKV-O-ALL		
44	3,7928E-11	00,03	Q4-POS0	Q4-S1	YT11Z01-PIP-T		
45	3,7928E-11	00,03	Q4-POS0	Q4-S1	YT11Z01-PIP-T		
46	3,2714E-11	00,03	Q4-POS0	EQ-Q4-YT11-005	Q4-S1		
47	3,1331E-11	00,03	Q4-POS0	Q4-S1	TQN0B01-BST-Q-ABC		
48	2,7336E-11	00,02	Q4-POS0	EQ-Q4-YT12-006	Q4-S1		
49	2,7336E-11	00,02	Q4-POS0	EQ-Q4-YT13-007	Q4-S1		
50	2,7336E-11	00,02	Q4-POS0	EQ-Q4-YT12-006	Q4-S1		
51	2,7336E-11	00,02	Q4-POS0	EQ-Q4-YT11-005	Q4-S1		
52	2,7336E-11	00,02	Q4-POS0	EQ-Q4-YT14-008	Q4-S1		
53	2,7336E-11	00,02	Q4-POS0	EQ-Q4-YT13-007	Q4-S1		
54	2,7336E-11	00,02	Q4-POS0	EQ-Q4-YT14-008	Q4-S1		
55	2,7336E-11	00,02	Q4-POS0	EQ-Q4-YT11-005	Q4-S1		
56	2,6571E-11	00,02	Q4-POS0	EQ-A1-YT11-005	Q4-S1		

MCS Analysis Case (Filtered)

ID Char #:1	Description	Calculati
L1-QS	S1, S2, S3 due to Q4 (0.3g) / Aftershock A1 (0.17g)	F

Analysis | Results

Importance for Basic Event

No	ID	Normal value	FV	FC
1	Q4-POS0	2,0000E-05	1,0000E+00	1,0000E+00
2	Q4-S1	3,3000E-01	8,2067E-01	8,2067E-01
3	EQ-Q4-YT13-007	5,1100E-02	4,3044E-01	4,3044E-01
4	EQ-Q4-YT14-008	5,1100E-02	3,0075E-01	3,0075E-01
5	EQ-Q4-YT12-006	5,1100E-02	2,9781E-01	2,9781E-01
6	YT11Z01-PIP-T	7,0900E-02	2,2567E-01	2,2567E-01
7	EQ-Q4-YT11-005	5,1100E-02	2,2222E-01	2,2222E-01
8	Q4-S3	9,5400E-02	1,2264E-01	1,2264E-01
9	YT12Z01-PIP-T	2,6800E-02	8,5303E-02	8,5303E-02
10	YT14Z01-PIP-T	2,5800E-02	8,2120E-02	8,2120E-02
11	EQ-Q4-CKV2-P2300	7,7160E-04	6,3192E-02	6,3192E-02
12	EQ-Q4-CKV2-P1920	7,7160E-04	6,3192E-02	6,3192E-02
13	Q4-S2	4,4200E-02	5,6682E-02	5,6682E-02
14	QS-A1	5,0000E-01	2,0987E-02	2,0987E-02
15	YT13-TM	1,7700E-03	1,4959E-02	1,4959E-02
16	EQ-A1-YT13-007	4,5490E-03	1,0479E-02	1,0479E-02
17	YT14-TM	1,7700E-03	1,0467E-02	1,0467E-02
18	YT12-TM	1,7700E-03	1,0365E-02	1,0365E-02
19	YT11-TM	1,7700E-03	7,7469E-03	7,7469E-03
20	EQ-Q4-CKV5-P0	6,9220E-05	5,6689E-03	5,6689E-03
21	EQ-A1-YT14-008	4,5490E-03	4,7064E-03	4,7064E-03
22	EQ-A1-YT12-006	4,5490E-03	4,5755E-03	4,5755E-03
23	EQ-Q4-CKV2-P1320	7,7160E-04	2,9165E-03	2,9165E-03
24	EQ-Q4-MOV1-P1320	7,7160E-04	2,8723E-03	2,8723E-03
25	YA30Z01C-PIP-T	1,3200E-01	2,4871E-03	2,4871E-03
26	YA10Z01C-PIP-T	1,3200E-01	1,7255E-03	1,7255E-03
27	EQ-Q4-TQ11-168	3,6210E-02	1,5952E-03	1,5952E-03
28	YT1NS0N-MOV-E-ALL	2,5369E-05	1,4600E-03	1,4600E-03
29	EQ-A1-YT11-005	4,5490E-03	1,2110E-03	1,2110E-03
30	YA40Z01C-PIP-T	1,3200E-01	1,2071E-03	1,2071E-03
31	EQ-A1-CKV2-P2300	2,0880E-05	8,5500E-04	8,5500E-04
32	EQ-A1-CKV2-P1920	2,0880E-05	8,5500E-04	8,5500E-04
33	YT1NS04-CKV-O-ALL	9,0060E-06	7,3756E-04	7,3756E-04
34	YT1NS03-CKV-O-ALL	9,0060E-06	7,3756E-04	7,3756E-04
35	EQ-Q4-TQ23-068	1,8600E-02	6,9984E-04	6,9984E-04
36	EQ-Q4-TQ23-080	1,8600E-02	6,9984E-04	6,9984E-04
37	EQ-Q4-TQ23-062	1,8600E-02	6,9984E-04	6,9984E-04
38	EQ-Q4-TQ23-065	1,8600E-02	6,9984E-04	6,9984E-04
39	YT13S03-CKV-O	8,1054E-05	6,8055E-04	6,8054E-04
40	YT13S04-CKV-O	8,1054E-05	6,8055E-04	6,8054E-04
41	YT14S04-CKV-O	8,1054E-05	4,7483E-04	4,7483E-04
42	YT14S03-CKV-O	8,1054E-05	4,7483E-04	4,7483E-04
43	YT12S03-CKV-O	8,1054E-05	4,7017E-04	4,7017E-04
44	YT12S04-CKV-O	8,1054E-05	4,7017E-04	4,7017E-04
45	YT11S04-CKV-O	8,1054E-05	3,4982E-04	3,4982E-04
46	YT11S03-CKV-O	8,1054E-05	3,4982E-04	3,4982E-04
47	YT13Z01-PIP-T	9,7000E-05	3,0784E-04	3,0784E-04
48	TQN0B01-BST-Q-ABC-	4,7472E-06	2,7321E-04	2,7321E-04
49	TQN0S02-CKV-O-ALL	2,8724E-06	2,3524E-04	2,3524E-04
50	TQ33D01-MDP-R	6,5444E-03	2,1885E-04	2,1885E-04
51	TQ23D01-MDP-R	6,5444E-03	2,1885E-04	2,1885E-04

Figure A.8: Results of analysis using the RiskSpectrum PSA testing model

2 Test modeling of aftershocks considering "intermediate damage state" of SSCs

The next step in the test modeling of aftershock was to consider the weakened "intermediate damage state" caused by the mainshock for critical SSCs of Zaporizhzhia NPP Unit 1, which make the highest contribution to CDF according to the test calculations using the SAPHIRE and RiskSpectrum PSA software tools (Figs. A.4, A.8). Accordingly, the following events were selected:

1) Failure of equipment group: instrumentation and control (I&C) systems and thermomechanical equipment:
   - SDS-P1320: failure of equipment group SDS located at elevation 13.2 m – I&C equipment of the primary process protections system;
   - CKV2-P1320: failure of equipment group CKV2 located at elevation 13.2 m – check valves on the lines of the emergency and regular core cooldown system and emergency boron injection system;
   - MOV1-P1320: failure of equipment group MOV1 located at elevation 13.2 m – electrically driven check valves on the lines of the emergency and regular core cooldown system;
2) Break/leak of the hydroaccumulator–reactor connecting piping:
   - YT11-005 (YT12-006, YT13-007, YT14-008): break/leak of the hydroaccumulator–reactor connecting piping on the section from hydroaccumulator YT11B01 (YT12B01, YT13B01, YT14B01) to valve YT11S02 (YT12S02, YT13S02, YT14S02);
   - YT11Z01-PIP-T (YT12Z01-PIP-T, YT14Z01-PIP-T): break/leak of the hydroaccumulator–reactor connecting piping on the section from valve YT11S02 (YT12S02, YT14S02) to the reactor pressure vessel incut.

For the identified critical SSCs, the fragility curves were recalculated taking into account the "intermediate damage state".

As stated in Chapter 2 of this Strategy, SSC damage/failure state largely depends on the site seismic level (levels of mainshocks and aftershocks considered). Therefore, to obtain representative results in the calculation of fragility curves considering the "intermediate damage state" of SSCs and subsequent test modeling of the aftershock, different combinations of seismic levels were analyzed (see Fig. A.9-A.12 and Tables A.1-A.4 below).

The influence of the weakened "intermediate damage state" caused by the mainshock on the reactor compartment building was considered separately. Initiating event Q-RB "Loss of the load-bearing capacity of the reactor compartment building resulting from seismic impact" directly leads to core damage and release.

2.1 Calculation of fragility curves considering "intermediate damage state" of SSCs

To plot the fragility curves for SSCs, the shift-based approach was used as proposed in para. 2.2.2 of this Strategy. According to this approach, the fragility curve of aftershock will shift to the left side of the fragility curve of mainshock because of the SSC structural damage caused by the mainshock and lower intensity of the aftershock.

Seismic resistance evaluation was performed previously using the seismic margin assessment (SMA) for SSCs of Zaporizhzhia NPP Unit 1 and SSC HCLPF values were obtained. In this regard, a combined (hybrid) method was employed to calculate the SSC fragility curves within the Zaporizhzhia NPP SPSA, where the median resistance of SSCs to seismic effects is determined through HCLPF of respective components /EPRI 1019200/:

$$A_m = \mathrm{HCLPF} \cdot e^{1{,}65(\beta_U + \beta_R)}.$$

Therefore, the shift factor of the SSC fragility curves will be determined by the decrease in HCLPF of SSCs in the weakened "intermediate damage state" caused by the mainshock.

In turn, HCLPF is calculated within SMA through the seismic margin factor (safety factor) FS:

$$HCLPF = FS \cdot F\mu \cdot PGA_{RLE} \qquad FS = \frac{C - D_{NS}}{\sqrt{(D_S^2 + D_{SAM}^2)} + \delta C_S}$$

where:

- F_μ – inelastic energy absorption coefficient (reference value)
- C – value of all allowable stresses
- D_{NS} – contribution of all non-seismic loads
- D_S – contribution of seismic inertial loads
- D_{SAM} – contribution of seismic displacement of supports
- δC_S – decrease of allowable stresses through seismic loading

Since the seismicity of the Zaporizhzhia NPP site (PGA_{SSE}=0.17g) is low and only the mainshock was considered in the previous seismic resistance assessment of SSCs at Zaporizhzhia NPP Unit 1, D_{SAM} and δCS were assumed to be zero:

$$FS = {}^{(C - D_{NS})}/_{D_S}$$

At the same time, structural damage to SSCs caused by the mainshock, provided that they retain a certain level of serviceability, leads to a decrease in the allowable stresses in SSCs and, accordingly, to a decrease in the seismic margin factor because of the need to account for δCS:

$$FS = \frac{C - D_{NS}}{D_S + \delta C_S}$$

For practical test calculations of the HCLPF value for SSCs in the weakened "intermediate damage state", the degree of this damage is postulated to be equal to the product of allowable stresses C to probability of SSC failure caused by the mainshock:

$$\delta C_S \equiv \mathrm{C} \cdot P_f(PGA_{MS}),$$

where the probability of SSC failure caused by the mainshock is determined from the fragility curves for non-weakened SSCs.

Examples of the calculated shift-fragility curves for the previously identified critical SSCs at ZNPP Unit 1, considering their "intermediate damage state" caused by the mainshock of the specific intensity according to the above approach, are shown in Figs A.9-A.12.

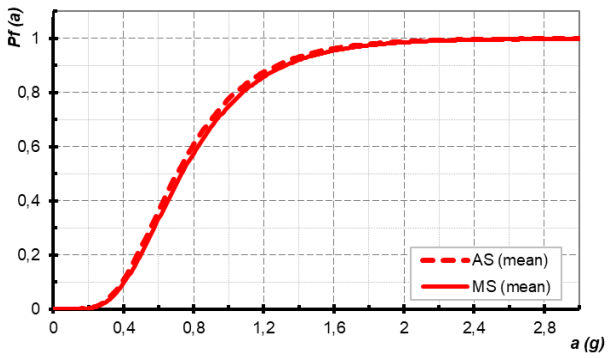

Combination 1 (MS 0.3g; AS 0.17g)

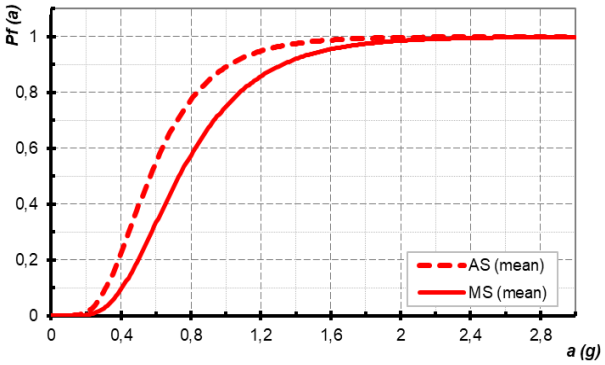

Combination 2 (MS 0.5g; AS 0.3g)

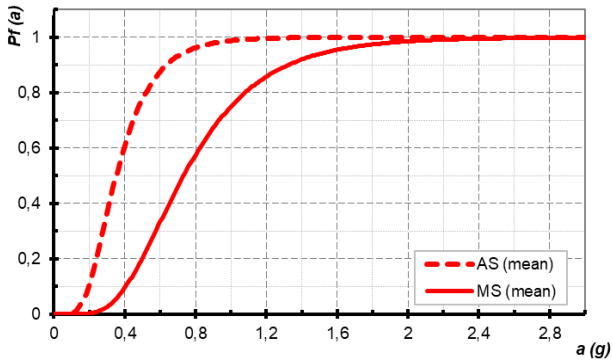

Combination 3 (MS 1.0g; AS 0.5g)

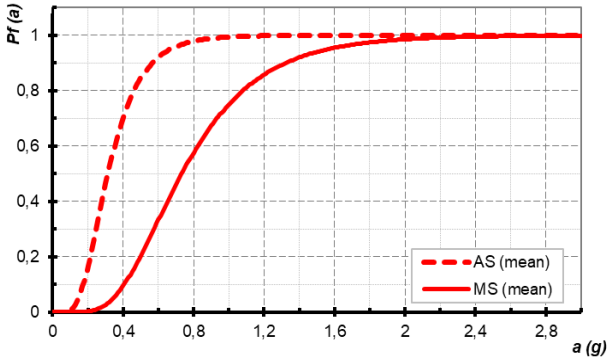

Combination 4 (MS 1.45g; AS 1.0g)

Figure A.9: Reactor building

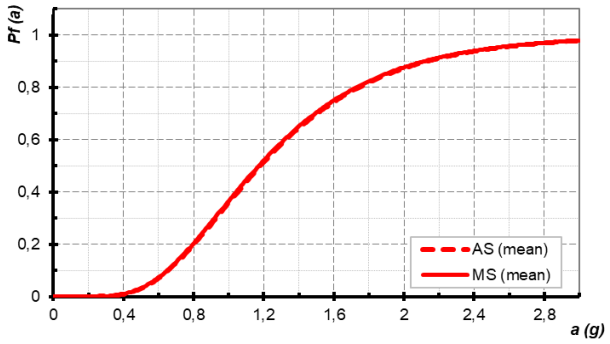

Combination 1 (MS 0.3g; AS 0.17g)

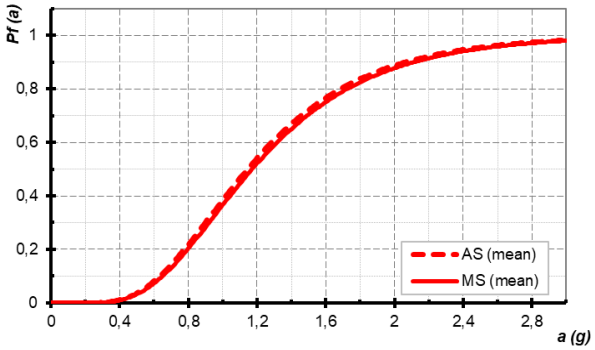

Combination 2 (MS 0.5g; AS 0.3g)

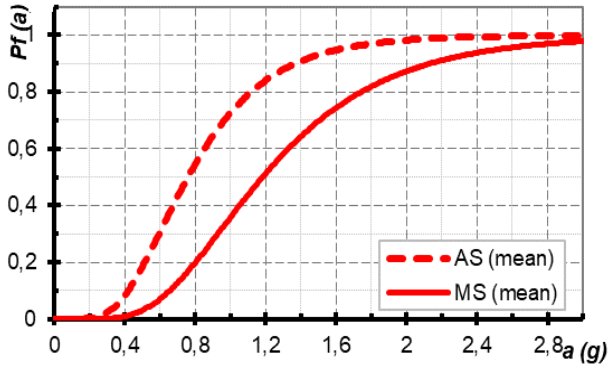

Combination 3 (MS 1.0g; AS 0.5g)

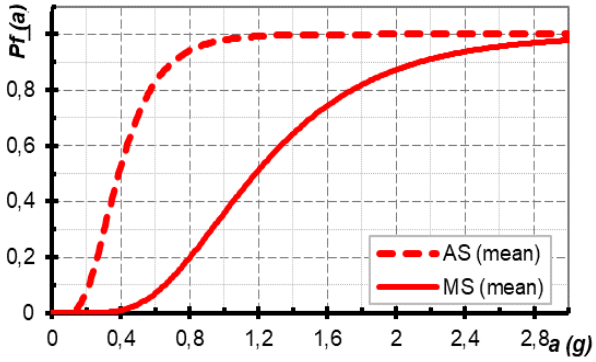

Combination 4 (MS 1.45g; AS 1.0g)

Figure A.10: Instrumentation and control equipment of primary process protection systems

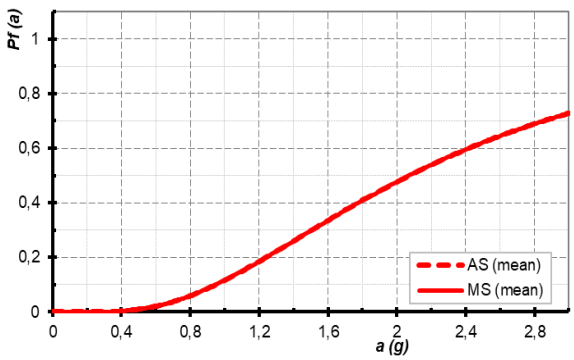

Combination 1 (MS 0.3g; AS 0.17g)

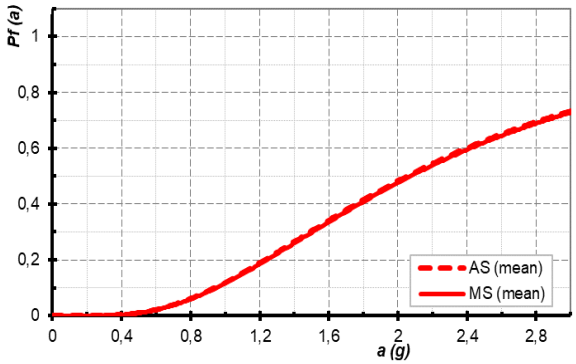

Combination 2 (MS 0.5g; AS 0.3g)

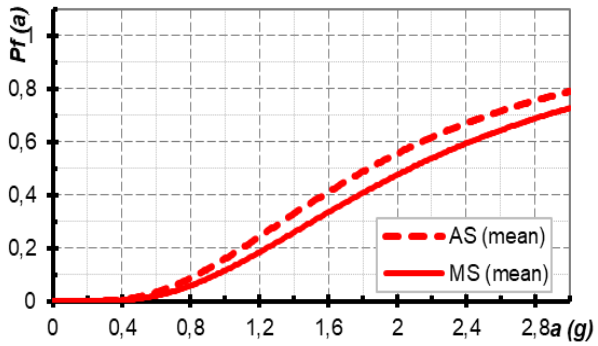

Combination 3 (MS 1.0g; AS 0.5g)

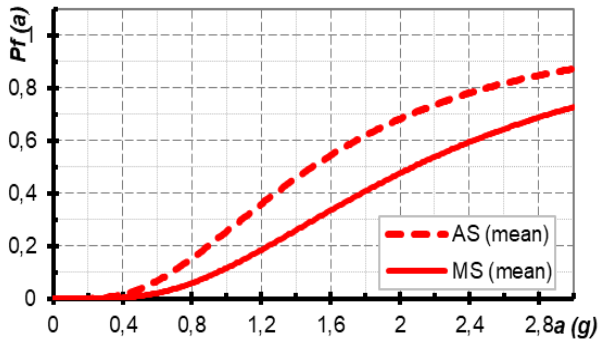

Combination 4 (MS 1.45g; AS 1.0g)

Figure A.11: Electrically driven check valves on lines of the emergency and regular core cooldown system

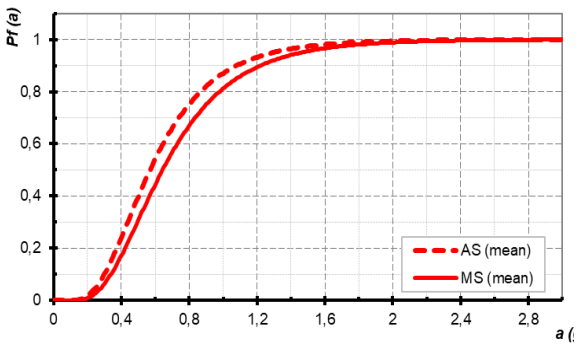

Combination 1 (MS 0.3g; AS 0.17g)

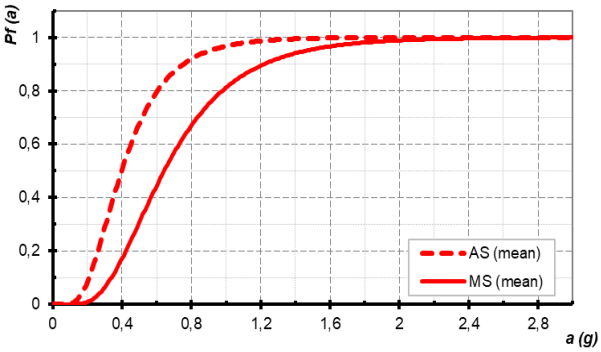

Combination 2 (MS 0.5g; AS 0.3g)

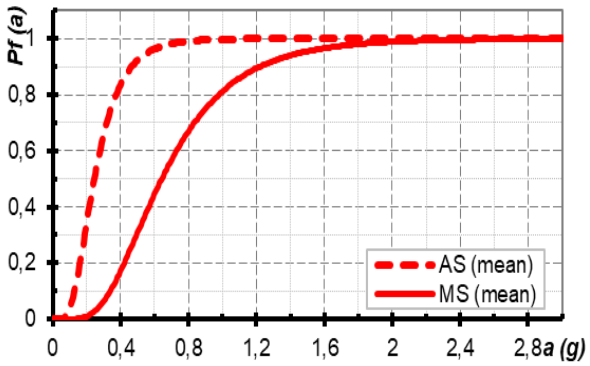

Combination 3 (MS 1.0g; AS 0.5g)

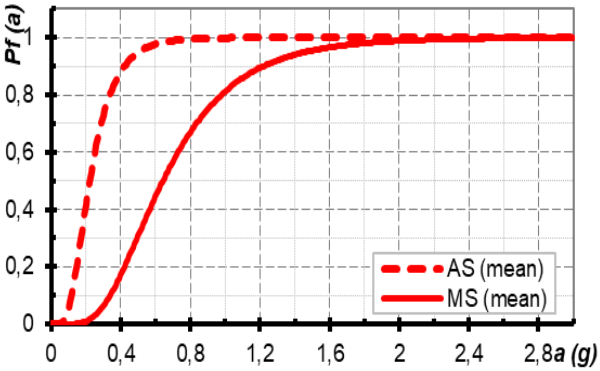

Combination 4 (MS 1.45g; AS 1.0g)

Figure A.12: Hydroaccumulator–reactor connecting piping on the section from valve YT11S02 (YT12S02, YT14S02) to the reactor pressure vessel incut

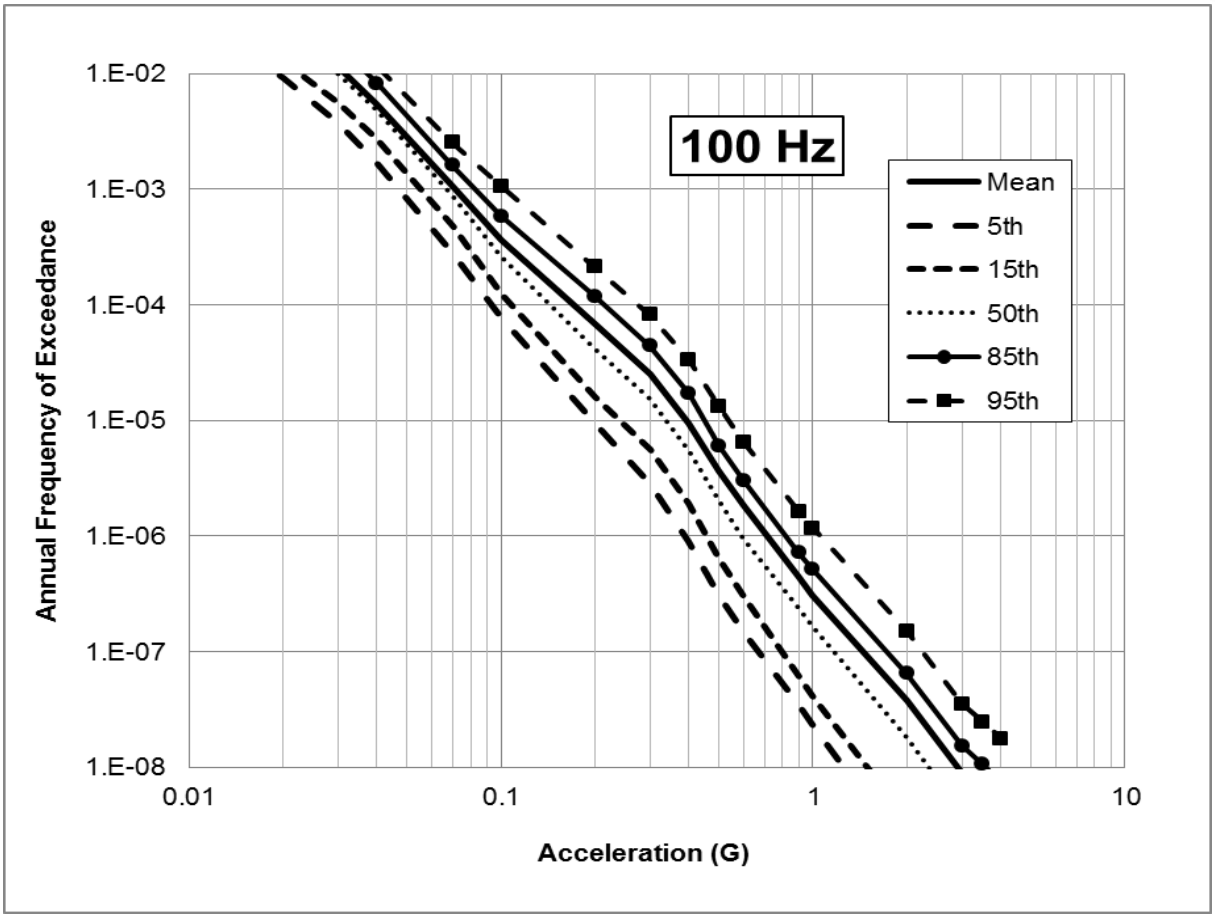

Figure A.13: ZNPP site seismic hazard curve

2.2 Example of aftershock modeling for the reactor compartment building

Initiating event Q-RB "Loss of the load-bearing capacity of the reactor compartment building resulting from seismic impact" directly leads to the reactor core damage. Therefore, the test calculation was performed without modeling using the SAPHIRE and RiskSpectrum PSA software tools.

For test calculation to determine the influence of aftershock on CDF considering the "intermediate damage state" of the ZNPP Unit 1 reactor compartment building, the following combinations of seismic effects were addressed:

Combination 1

- mainshock Q4 with PGA=0.3g and 2.51E-05 frequency;
- aftershock with PGA=0.17g and 5.00E-01 postulated probability after the mainshock.

MS	AS	AS_Shift	Δ AS
CDFrb=f*Pms	CDFas=0.5*f*(1-Pms)*Pas	CDFas_sh=0.5*f*(1-Pms)*Pas_shift	
6.65E-07	9.42E-09	1.25E-08	3.04E-09
100	1.41%	1.87%	0.46%

Table A.1: Results for combination 1 (MS=0.3g; AS=0.17g)

Combination 2

- mainshock Q0.5 with PGA=0.5g and 3.61E-06 frequency;
- aftershock with PGA=0.3g and 5.00E-01 postulated probability after the mainshock.

MS	AS	AS_Shift	Δ AS
CDFrb=f*Pms	CDFas=0.5*f*(1-Pms)*Pas	CDFas_sh=0.5*f*(1-Pms)*Pas_shift	
7.36E-07	3.81E-08	1.22E-07	8.35E-08
100	5.17%	16.51%	11.34%

Table A.2: Results for combination 2 (MS=0.5g; AS=0.3g)

Combination 3

- mainshock Q1.0 with PGA=1.0g and 3.09E-07 frequency;
- aftershock with PGA=0.5g and 5.00E-01 postulated probability after the mainshock.

MS	AS	AS_Shift	Δ AS
CDFrb=f*Pms	CDFas=0.5*f*(1-Pms)*Pas	CDFas_sh=0.5*f*(1-Pms)*Pas_shift	
2.32E-07	7.86E-09	2.99E-08	2.21E-08
100	3.39%	12.90%	9.51%

Table A.3: Results for combination 3 (MS=1.0g; AS=0.5g)

Combination 4

- mainshock Q5 with PGA=1.45g and 1E-07 frequency;
- aftershock with PGA=1.0g and 5.00E-01 postulated probability after the mainshock.

MS	AS	AS_Shift	Δ AS
CDFrb=f*Pms	CDFas=0.5*f*(1-Pms)*Pas	CDFas_sh=0.5*f*(1-Pms)*Pas_shift	
9.31E-08	2.59E-09	3.43E-09	8.39E-10
100	2.78%	3.68%	0.90%

Table A.4: Results for combination 4 (MS=1.45g; AS=1.0g)

In Tables A.1-A.4, column Δ AS shows the effect (in percent) of the weakened "intermediate damage state" caused by the mainshock of the ZNPP Unit 1 reactor compartment building and subsequent aftershock on CDF. Other symbols: f is the frequency of mainshock (PGA) occurrence (see Fig. A.13) and Pms, Pas, and Pas_shift are the probabilities of SSC failure due to the mainshock and aftershock, respectively.